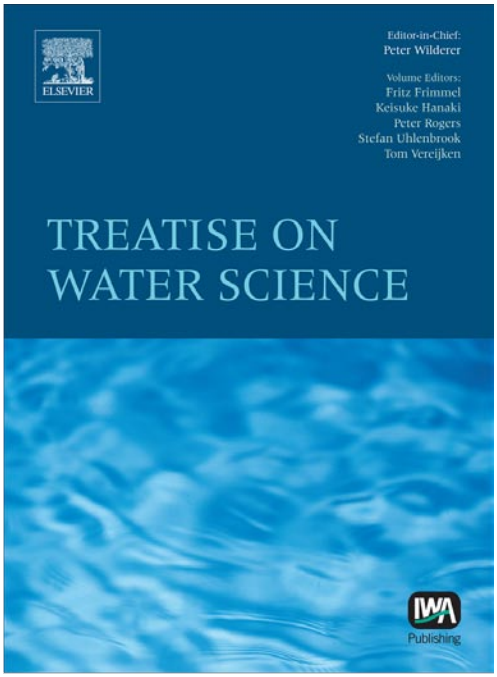

Orellana G, Cano-Raya C, López-Gejo J and Santos AR (2011) Online Monitoring Sensors. In: Peter Wilderer (ed.) Treatise on Water Science, vol. 3, pp. 221–262 Oxford: Academic Press.

3.10 Online Monitoring Sensors

G Orellana, C Cano-Raya, J López-Gejo, and AR Santos, Complutense University of Madrid, Madrid, Spain

3.10.1 Introduction

Nowadays, sensors are regarded as the electronic mimics of the human senses. Thanks to both physical and chemical sensors, we can constantly be aware of natural and human-made phenomena. In this way, it is possible to monitor the status of watercourses, oceans, underground aquifers, water-treatment plants, distribution networks, etc., and take corrective actions as early as possible, before any damage is inflicted. This chapter provides an overview of the currently available sensors for water-quality monitoring and analysis.

The definition of a sensor includes any device that is able to provide a measurement of a physical parameter (e.g., turbidity and conductivity), or the concentration of a chemical

species (e.g., molecular oxygen, ions, toxins, and hydrocarbons) *in situ*, in real time and continuously. *In situ* implies that the monitoring device can be taken to the point of measurement and introduced directly into the target water body (e.g., a pH meter), or placed where sampling and analysis can be made without human intervention. Nevertheless, the sensor signal can be sent far away from the monitoring site to central sites where the actual control is located and decisions are made. Currently, in use are radio, global system for mobile connections (GSM), and satellite links. Real-time monitoring involves rapid response by the sensor to changes in the monitored parameter, so that immediate action can be taken if needed. However, while this is the ideal behavior of any sensing device, there are processes such as analysis of several chemical species (e.g., waterborne organic matter) that require sample pretreatment. The true sensor must perform this operation *in situ* and online at the expense of a longer response time. Despite this, the sensor response is much shorter than the time taken to perform manual sampling, which involves transport of samples to the laboratory and subsequent analysis. Continuous measurements imply that the sensor response is reversible (ideal situation) or, at least, it can be regenerated *in situ* without human intervention. The devices that do not fulfill this last feature are often called 'dosimeters', although many scientific and commercial publications also refer to them as 'sensors'.

This chapter is intentionally restricted to true sensors, that is, devices that meet the three requirements mentioned earlier. However, where commercially available online sensors are not accessible for an important water-quality parameter, or when manual tests are firmly established in the water-monitoring field, the corresponding dosimeters are briefly described.

The dynamic range of an analyzer is normally regarded as the analyte-concentration interval that the instrument is able to measure in an effective manner, that is, from the detection limit to the maximum usable indication. The detection limit refers to the smallest amount of substance or element detectable by the sensing device (typically corresponding to an analytical signal equal to 3 times the standard deviation of the background noise). From the statistical point of view, the limit of determination is always higher than the limit of detection of the sensor. Therefore, even though many manufacturers state that a particular sensor for water monitoring is applicable within an analyte concentration range from 0 to x (units), it must always be understood that the lowest indication value is actually the limit of detection.

Given the wide variety of chemical sensors developed for water monitoring and the different types of sampled waters (natural, potable, underground, industrial, recreational, recycled, wastewaters, etc.), it is impossible to provide a general critical view on the practical applicability of these devices. Nevertheless, a critical assessment of the advantages/disadvantages of the different sensors described in this chapter is included under each section.

3.10.2 Sensors for pH Measurements

The acidity of water is probably the most widespread chemical parameter measured in both environmental and industrial fields. In this section, we describe pH sensors divided into two main groups, namely electrochemical and optical devices.

3.10.2.1 Electrochemical pH Sensors

The potentiometric measurement of pH is based on the electrochemical cell:

Reference electrode|concentrated KCl||test solution
|electrode reversible to $H^+(aq)$

where, typically, the electrode reversible to hydrogen ions is a glass electrode that is assumed to exhibit Nernstian behavior. The electromotive force (emf) of this cell is given by the expression

$$E = E^{0'} + k_N \log\{H^+\} + E_j \qquad (1)$$

where k_N is the Nernst constant ($RT\ln 10/F$), $\{H^+\}$ is the thermodynamic activity of the hydrogen ions, E_j is the liquid junction potential that arises from the ionic strength differences between the electrolyte solution of the reference electrode and the test solution, and $E^{0\prime}$ is the conditional potential of the cell which depends on the experimental conditions (such as the filling solution) in the pH electrode and the contribution of the reference electrode potential. During routine measurements, electrode readings in one or more reference solutions are compared to that of the test solution. Assuming that the E_j values in both the test and the reference solution are the same ($\Delta E_j = 0$), the pH of the test solution is, therefore, operationally defined as

$$pH(X) = pH(S) + (E_S - E_X)/k_N \qquad (2)$$

where X and S indicate the test and reference solution, respectively.

3.10.2.1.1 pH electrodes based on redox reactions

There are two types of indicator electrodes: metal- and carbon-based. Metal electrodes develop an electric potential in response to a redox reaction at the metal surface. The most common metal indicator electrode is made of platinum, which is relatively inert. An advantage of the metal oxide electrodes is that they have very low resistance, but may be subject to severe interference by redox reactions.

Various types of carbon can be used as pH electrodes because the rates of many redox reactions on the carbon surface are fast enough. Although many such materials respond to pH without preliminary activation, the derivatization of carbon surfaces has allowed development of electrodes for pH measurements that offer advantages compared to other pH meters (Kahlert, 2008).

3.10.2.1.2 Ion-selective electrodes for pH measurements

Ion-selective electrodes are different from metal electrodes in that the former do not depend on redox processes. The essential feature of an ideal ion-selective electrode is a thin membrane across which only the target ion can migrate. The most important ion-selective electrodes for pH determination

are glass electrodes, liquid membrane electrodes, and ion-sensitive field-effect transistors (ISFETs).

Glass pH electrode. The glass pH electrode used to measure water acidity is the most common example of an ion-selective electrode. The overall galvanic cell of a typical (combination) glass electrode incorporating both glass and reference electrodes can be represented by

Reference electrode (internal)	H^+ (internal)	Glass membrane	H^+ (external) analyte	Reference electrode (external)

Glass electrode

The key to electrode selectivity lies in its glass membrane. The surface layers of the latter consist of fixed silicate groups associated with sodium ions ($-OSiO_2^-Na^+$). When this electrode is dipped in water, the sodium ions exchange with the solvated protons in water and the surface is then described as 'hydrated'. The glass membrane has an inner and outer hydrated layer. In these hydrated layers, the anion sites are covalently bound to the bulk of the glass and are fixed. However, the H^+ cations are mobile, being free to exchange with the external solution or with sodium ions in the body of the glass. When the electrode is placed in an aqueous solution of unknown pH, the activity of the H^+ ions in the test solution is likely to be different from the activity of the H^+ ions in the hydrated layer. This sets up a potential difference between the solution and the surface of the membrane. This boundary potential is determined by this difference in the activities.

Beckman marketed the first pH glass electrode and meter in 1935. The glass pH electrode system used nowadays consists of a pH-sensitive measurement glass electrode and a separate reference electrode in a potassium chloride (KCl) gel-conducting solution (**Figure 1**). These electrodes are usually housed in the combination sensor, containing both electrodes, which is connected to an electronic meter with a signal amplifier and temperature compensation. The meter displays the pH reading, which may be uploaded to a computer or controller. A silver wire enclosed in the measurement electrode forwards a signal indicating the difference in acidity between the solutions inside and outside the glass membrane. The reference electrode has a stable potential, which is independent of the measuring solution and must be calibrated outside the system in a reference solution. The most commonly used reference is a silver/silver chloride electrode in a buffer. The measurement and reference electrodes complete a circuit through the water sample (via a permeable porous junction built in the glass wall, **Figure 1**) allowing measurements of the voltage generated by the glass electrode.

Common glass pH electrodes are extraordinary sensors in that they operate within a typical temperature range of 0–90 °C over the full pH range of 0–14 (14 orders of magnitude of the H^+ concentration!), although they require accurate temperature measurement and compensation. The pH signal generated by a glass electrode can drift, or lose accuracy, over time due to a number of factors including fouling, sensor instability, and interference from external equipment. Therefore, accurate pH measurements require an external recalibration procedure using standard solutions of known pH. Other potential pitfalls of the pH glass electrodes include fragility, difficult miniaturization, leakage of the reference electrode buffer into the sample solution, poor response in low ionic strength solutions, high background noise, and moderate signal-to-noise ratio.

Liquid membrane pH electrodes. Liquid membrane pH electrodes (LMEs; including polymeric membrane electrodes) offer advantages over other types of pH sensors and their aquatic applications are promising. Their key component is a pH-sensitive membrane that contains a pH-selective material composed of a neutral proton carrier dissolved in a membrane solvent. The membrane solvent is not miscible with water forming an organic phase that separates the aqueous sample solution from the aqueous internal filling solution. The neutral carriers are capable of selectively extracting ions from aqueous solution into the membrane phase and transporting them across the organic phase by carrier translocation. Similarly to the glass electrode, a membrane potential is established during the process and can be measured against a reference electrode. Compared to glass pH electrodes, LMEs have shorter response times because of their lower inner resistance.

Ion-sensitive field-effect transistors. The ISFET is an integrated device containing an ion-selective electrode and an insulated-gate field-effect transistor. In pH-sensitive FETs, the ion-selective layer consists of SiO_2, Si_3N_4, Ta_2O_5, or Al_2O_3, currently Ta_2O_5 being the preferred pH-sensitive layer. Technical difficulties regarding the required encapsulation of the electronic components due to their sensitivity to moisture are the main problems of ISFET fabrication. These problems have been solved by advanced packaging technologies so that an

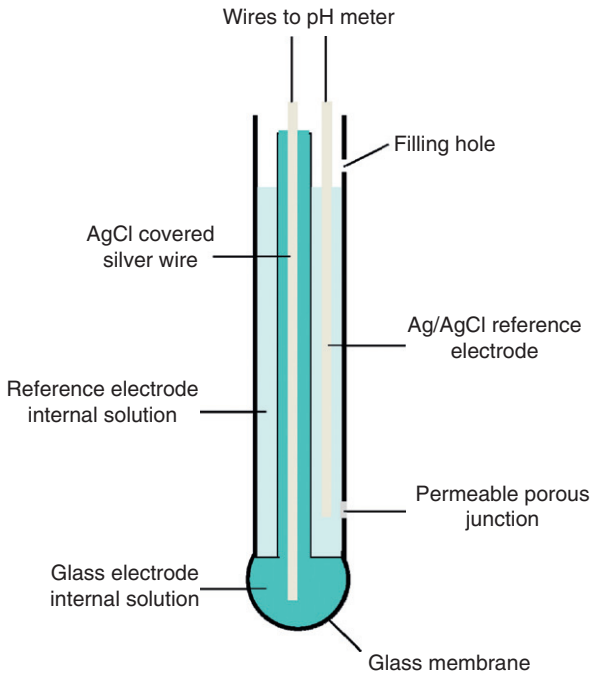

Figure 1 Typical glass electrode for pH measurements.

economical mass production of solid pH sensors is possible. The major problems that persist are in finding a compatible reference electrode and avoiding hysteresis effects. Nevertheless, ISFETs are sensitive over a wide pH range (0–14) and are able to measure faster and with less temperature dependence than glass electrodes. Unlike the latter, ISFET-based pH sensors possess a rugged structure, small size, and low impedance, being amenable to miniaturization and automation. Moreover, ISFETs are not expected to be sensitive to organic contaminants and redox species in natural environments. Representative electrodes for pH sensing are listed in Table 1.

3.10.2.2 Optical pH Sensors

Optical pH sensors, also known as pH optodes, are based on pH-dependent variations in the optical properties of an indicator dye, which reacts reversibly with the protons or bases in the aqueous sample. The most popular designs use the pH-dependent absorption or fluorescence of reagents that are weak electrolytes and exist in both acidic and basic forms over the pH range of interest (typically *c.* 4 units). The acid (hyaluronic **acid** (HA)) and the corresponding conjugated base (A^-) participating in the pH-dependent chemical equilibrium are selected to have different absorption or fluorescent properties:

$$\mathrm{HA\ (color\ A)} \rightleftharpoons \mathrm{H^+ + A^-(color\ B)} \tag{3}$$

Since the degree of dissociation depends on the solution pH, the acidity level can be determined by measuring the relative concentrations of both forms of the dye. It is important to point out that most reports on pH optodes ignore the effect of ionic strength on the dissociation equilibrium of the indicator. While this omission is acceptable in dilute solutions, it can lead to serious errors in some environments.

Absorption- and reflectance-based pH sensors. Absorption-based pH sensors operate under the Beer–Lambert law that relates the absorbance at the analytical wavelength (A_λ) of an aqueous solution of the indicator dye to the concentration (C) of its acidic and basic forms (Equation (4)):

$$A_\lambda = \log\frac{P_{0,\lambda}}{P_\lambda} = \varepsilon_\lambda(\mathrm{HA})lC_{\mathrm{HA}} + \varepsilon_\lambda(A^-)lC_{A-} \tag{4}$$

where $P_{0,\lambda}$ and P_λ represent the incident and transmitted spectral radiant power at the analytical wavelength of the monochromatic radiation used to interrogate the system, respectively; l is the absorption path length and ε_λ is the molar absorption coefficient at the analytical wavelength of the acidic and basic species of the indicator dye. The measured absorbance is a function of the solution pH due to the effect of the latter on the acid/base equilibrium of the indicator dye.

For practical fabrication of optical pH-meters, the indicator dye is usually immobilized onto a polymer support and interrogated using optical fibers to carry the light to and from the distal end where the sensing head is placed. If the supported dye is in particulate form rather than a film, it needs to be confined and separated from the sampled water by a H^+-permeable membrane. The Beer–Lambert law also holds in transparent polymer supports but, if the indicator dye is adsorbed onto opaque materials, then diffuse reflectance rather than absorbance must be measured. In this case, the Kubelka–Munk function, that relates the absolute diffuse reflectance of the indicator material at the analytical wavelength (R_λ) to the concentration of the immobilized absorbing species (C), is used:

$$f(R) = \frac{(1-R_\lambda)^2}{2R} = \frac{2.303\varepsilon_i C}{S_\lambda} \tag{5}$$

where ε_λ has been defined above and S_λ is the scattering coefficient of the indicator support material at the analytical wavelength. The latter is assumed to be independent of the immobilized dye concentration. As in the case of absorption-based pH sensors, the overall dye concentration will be distributed among its acidic and basic forms (Equation (3)) depending on the pH. Therefore, the diffuse reflected color intensity at the chosen analytical wavelength will be a function of the sampled water pH.

Fluorescence-based pH sensors. Fluorescence is particularly well suited for optical sensing due to the high sensitivity and selectivity of the emission phenomenon. For weakly absorbing solutions ($A_\lambda < 0.05$), the fluorescence intensity at the analytical wavelength ($I_{F,\lambda}$) returning from the sensing head is directly proportional to the intensity of the exciting radiation (I_0) and to the concentration of the fluorescent dye (C) in the sensor:

$$I_F = k' I_0 \Phi \varepsilon_i l C \tag{6}$$

where l is the absorption path length through the sensing layer, ε_λ is the molar absorption coefficient, Φ is the fluorescence quantum yield, and k' is the fraction of the fluorophore emission that can be measured in each particular setup. Fluorescent indicator molecules are also immobilized onto a polymer support and the emission from the fluorescent material is a function of the sample pH due to the dependence of the indicator acidic and basic forms concentration on that parameter.

Absorption versus fluorescence pH sensors. Absorption measurements are simple and easy to use but are not very sensitive, requiring the use of high concentrations of pH indicator dye and/or a thick sensing layer. Reflection configurations with bifurcated fiber bundles are often used to overcome this problem. In contrast, fluorescent measurements are much more sensitive and can be used for small-size sensors and/or low indicator concentration.

Fluorescent sensors can be operated in the (absolute) emission intensity mode and/or the emission lifetime mode, depending on whether steady-state or pulsed excitation of the indicator dye is performed. Fluorescence lifetimes can also be determined by sinusoidally modulating the excitation light and measuring the (sinusoidally) modulated emission phase shift. The current light-emitting diodes (LEDs) have helped to make the latter method very popular. Sensors based on fluorescence lifetime measurements are preferable because of their decisive advantages over absolute intensity recording: it is intrinsically self-referenced, it has negligible signal drift due to independence of the decay time with luminophore

Table 1 Some academic and commercial electrochemical sensors for pH determination

pH-sensitive electrode	*pH range*	*Slope (mV/pH unit)*	*Response time*	*Interferences*	*Lifetime*	*pH electrode type*	*References*
W/WO_3	3–6	−61.1	40 s	NA	NA	Redox	[a]
IrO_x	2–12	-64 ± 7	NA	Ni^{2+}	2 months	Redox	[b]
Functionalized graphite	NA	−59	2–3 s	NA	NA	Redox	[c]
Functionalized carbon black	2–7	−59	NA	NA	NA	Redox	[d]
Functionalized glassy carbon	4–12	59	NA	NA	NA	Redox	[e]
Functionalized glassy carbon	1–11	55	NA	NA	NA	Redox	[f]
Functionalized glassy carbon	1–11	−54.7	10 min	NA	NA	Redox	[g]
Functionalized carbon epoxy	1–12	−60	60 s	NA	NA	Redox	[h]
Functionalized carbon, organic binder (silicone, PTFE)	0–9	−58	<2 s	NA	NA	Redox	[i]
Polypyrrole on PTFE	2–12	−37.8	50–100 s	NA	NA	Redox	[j]
Octyldibenzylamine	2–10 (2–55 °C)	56.5 (20 °C)	NA	Small effect of Na^+, K^+, Ca^{2+}	NA	LME	[k]
Glass	2–11	NA	Few seconds	NA	530 days	ISE	[l]
Ta_2O_5 film	2–12	55–58	NA	NA	NA	ISFET	[m]
Polyelectrolyte multilayers	4–9	39–42	NA	NA	NA	ISFET	[n]
NA	0–14 (0–95 °C)	NA	NA	NA	NA	Redox	[o]
Glass	0–14 (0–100 °C)	53–60	<30 s	Na^+	NA	ISE	[p]
Glass	1–12 (<80 °C)	NA	NA	NA	NA	ISE	[q]
Glass	0–14 (25 °C)	59	NA	NA	NA	ISE	[r]
Glass	0–14	NA	1–5 s	Na^+ error at pH > 12.3	NA	ISE	[s]
NA	0–14 (0–60 °C)	53.23 (25 °C)	NA	Hysteresis	6–12 months	ISFET	[t]
NA	0–14 (<135 °C)	NA	NA	NA	NA	ISFET	[u]

[a]Fenster *et al.* (2008).
[b]El–Giar *et al.* (2007).
[c]Szepesvary and Pungor (1971).
[d]Jankowska *et al.* (1981).
[e]Lawrence and Robinson (2007).
[f]Holm *et al.* (2007).
[g]Brown *et al.* (1976).
[h]Li *et al.* (2002).
[i]Scholz *et al.* (2005) and Kahlert *et al.* (2004).
[j]Prissanaroon *et al.* (2005).
[k]Cho *et al.* (1998).
[l]Kaden *et al.* (2004).
[m]Poghossian *et al.* (2003).
[n]Schöning *et al.* (2009).
[o]Continuously self-calibrating sensor (http://www.sensorin.com).
[p]Thermo Scientific (http://www.thermo.com).
[q]Orbisint Memosens Glass Electrode (http://www.emc.co.nz).
[r]pH/ORP monitor/controllers (http://www.myronl.com).
[s]Sensorex (http://www.sensorex.com).
[t]Argus ISFET (http://www.sentron.nl).
[u]Tophit-H Glassless Memosens (http://www.emc.co.nz).
NA, not available; PTFE, poly(tetrafluoroethylene).

concentration, and fluctuations in light-source intensities and photodetector do not influence the measurements.

3.10.2.3 Optical versus Electrochemical pH Sensors

The most significant advantage of spectrophotometric methods is their high precision. There are no liquid-junction or high-impedance problems with optical measurements, and calibration is inherent in prior knowledge of the thermodynamic properties of the indicator dye. However, interrogation of pH electrodes is simpler, and therefore electrochemical sensors are more economical than their optical counterparts. Moreover, the enormous dynamic range of the pH electrodes can never be beaten by the optical pH-meters. The latter can be a useful option when miniature sensors operating in a narrow pH range are needed, or when the optical sensing monitors developed successfully for other widespread water-quality parameters such as dissolved oxygen (see Section 3.10.5) can be directly used for pH measurements.

A summary of optical pH sensors for water appears in Table 2.

3.10.3 Sensors for Ionic Species

The monitoring of ionic species in water is of particular interest when considering drinking-water applications or, in general, public health. However, it is also relevant in other aspects of environmental analysis, such as aquatic life or industrial processes. The relative importance of monitoring the different waterborne ions depends on the particular nature of the aqueous medium. Aluminum compounds, for instance, can be found in swimming pools due to their use as flocculating agents, or in wastewater discharges from aluminum smelting where it becomes harmful to aquatic life. The presence of ammonium in groundwaters is an indication of potential pollution. Cadmium and lead ions are associated with the industrial production of batteries, while calcium and magnesium ions are responsible for water hardness. Chloride and bromide are ubiquitous and, in forced irrigation systems, groundwater can be monitored for these ions to avoid excess salinity. The presence of phosphates is important for plant life, as they are nutrients; yet if a wastewater rich in phosphate detergents is found due to insufficient monitoring, it produces environmentally damaging algal blooms. Another element essential to plant growth is sulfur, which can also be harmful to humans if present as sulfite ion, a potent allergenic species. Sulfite and hydrogen sulfide are often used to eliminate residuals of chlorine in wastewaters, due to the strong reducing potential of these ions. However, dissolved free sulfides strongly promote corrosion of many metals. Fertilizers are rich in nitrogen compounds such as nitrates that are harmful when they are found at high levels in water. Nitrites and nitrates can also be pollutants in aquarium waters. Both potassium and sodium cations are present in drinking, process, and wastewaters, their monitoring being relevant in the food industry as well as in horticulture as components of fertilizers. Several other ionic species (chromate, cobalt, copper, iron, lead, manganese, molybdenum, sulfate, zinc, nickel, tin, etc.) can also be found in water discharged from industrial areas.

Depending on the water to be monitored, the ion-concentration range may be very different. For example, according to the US Environmental Protection Agency (EPA), the highest concentration of arsenic to which an aquatic community can be exposed briefly without resulting in an unacceptable effect is $340\,\mathrm{mg\,l^{-1}}$. However, this value is limited to only $0.018\,\mathrm{mg\,l^{-1}}$ when considering waters for human consumption. It is obvious that a sensor system becomes more expensive with higher sensitivity, a factor that must be considered when evaluating the application needs.

Some waterborne ionic species can easily be transformed into neutral ones in the gas phase by just changing the pH of the sample, facilitating their determination by indirect methods. This is the case of sulfur compounds, chlorides, and ammonium. For instance, upon acidification of the water sample to be monitored, sulfite, hydrogen sulfide, and sulfide ions yield sulfur dioxide and hydrogen sulfide gases according to the following reactions:

$$SO_3^{2-} + 2H^+ \rightarrow SO_2(g) + H_2O$$

$$HS^- + H^+ \rightarrow H_2S(g)$$

$$S^{2-} + 2H^+ \rightarrow H_2S(g)$$

Obviously, the need for a pH change in the water sample requires more than a simple point-sensitive device. Moreover, many ion sensors require sample preconditioning. Therefore, manufacturers have developed total analytical systems containing fluidic tubing, peristaltic pumps, reagent reservoirs, sensing chambers, and cleaning devices that can be deployed *in situ* for continuous monitoring of waterborne ions. These systems require more frequent maintenance servicing than the simple sensors, and therefore are more expensive to operate. It has to be borne in mind that personnel costs are always much higher than the cost of any monitoring sensor network, a fact that must be carefully considered when evaluating the monitoring needs of a particular application.

Most of the devices for waterborne ionic-species monitoring rely on electrochemical processes for detection of the analyte, but there have emerged in the market, an increasing number of instruments based on optical-detection schemes, due to the advantages they offer. However, many commercial systems or devices described in the literature for ion sensing cannot be defined as true sensors (see Section 3.10.1), but are rather dosimeters because of their irreversible response. However, due to their widespread use, they have been included in this subsection to let the reader judge whether they can be useful for his/her particular application.

3.10.3.1 Ion-Selective Electrodes

Sensors based on electrical measurements (potentiometric, amperometric, and conductometric) are widely used for field applications due to their low cost, simplicity, and robustness. When available (see, for instance, Section 3.10.2), they allow

Table 2 Some optical pH sensors found in recent literature and commercial sources

Chemical reagent	*λ (nm)*	*pH range*	*Precision*	*Response time*	*Temperature range*	*Interferences*	*Lifetime*	*Transduction principle*	*References*
Thymol blue	435	Seawater pH	0.001 pH unit	NA	NA	NA	4 weeks	Absorption	[a]
p–Methyl red	540,	1.0–3.5	NA	15.8 s	1–3.5 °C	NA	NA	Absorption	[b]
4-CP-BPB	445, 606	2.0–6.0		11.9 s					
Bromocresol green	610	4.0–7.0	20% (RSD)	5 min	NA	NA	NA	Absorption	[c]
PoAnis/TSA	501	4.9–10.5	0.01 pH unit	5 min (acid to basic)	NA	Ionic strength (Na^+, Li^+, Cl^-)	NA	Reflectance	[d]
		2.0–10.0		5–22 min (basic to acid)					
Thymol blue	NA	6.8–9.5	NA	≤60 s	NA	NA	NA	Reflectance	[e]
Congo red		7.9–11.2							
Bromothymol blue		3.3–4.8							
Organometal-carbonyl complexes	2100–1750 cm^{-1}	7–13	NA	NA	NA	NA	NA	Reflectance	[f]
Swellable hydrogel	NA	4–5	NA	≤30 s	NA	NA	NA	Swelling-dependent reflectance	[g]
Langmuir–Blodgett film	750, 780	11–13	0.001–0.1	≈20 s	NA	NA	NA	Evanescent wave absorption	[h]
$[Ru(bpy)_2(dh\text{-}phen)]$ $(ClO_4)_2$	Exc. 415	1–8	≤0.11 pH unit	2–5 min	NA	Oxygen	2 weeks	Fluorescence	[i]
	Em. 612								
BNS, BrN/PhR, BCP, BPB	Exc. 300	3.5–9.2	≤0.5 pH unit	2 min	20 ± 3 °C	Cd^{2+}, Cu^{2+} ≤ 5 mg l^{-1}	2 m	Fluorescence (energy transfer)	[j]
	Em. 535								
HPTS	Exc. 405/450	6.5–8.5	NA	≤5 s	NA	Ionic strength	50 days	Fluorescence	[k]
	Em. 520								
TAPP/MBTD	Exc. 422/481	1.5–5.0	NA	≤60 s	NA	Ionic strength	1 month	Fluorescence	[l]
	Em. 656/528								
DHFA/DHFAE/ $Ru(dpp)_3$	Exc. 516/468/ 530/505	7.5–9.0	0.1 pH unit	≤230 s	21 ± 2 °C	Temperature	NA	Fluorescence	[m]
	Em. 540/554/600							DLR	
Mercurochrome	Exc. 506	1–9	0.01–0.06 pH unit	≈1 min	NA	Not found	8 months	Fluorescence	[n]
	Em. 530								
APN /MBTD	Exc. 393/479	5.80–8.80	NA	≈90 s	NA	Not found	1 month	Fluorescence	[o]
	Em. 524/530								

(*Continued*)

Table 2 Continued

Chemical reagent	*λ (nm)*	*pH range*	*Precision*	*Response time*	*Temperature range*	*Interferences*	*Lifetime*	*Transduction principle*	*References*
MAHPDS	Exc. 404/457 Em. 510	6.5–9.0	0.05 pH unit	≤216 s	NA	NA	NA	Fluorescence	[p]
HPTS	Exc. 406/460/506 Em. 515/540	5.5–8.6	NA	2 min	NA	NA	NA	Fluorescence	[q]
Phenol red	525	6.2–8.4	0.1	20 s	NA	Total alkalinity: 40–140 ppm	NA	Absorption	[r]
NA	NA	3.5–8.5	0.005 pH unit	<40 s	2–50 °C	Ionic strength fluorescent molecules	2 years	Fluorescence	[s]
Phenol red	NA	6.5–8.5	0.1	NA	NA	NA	NA	Absorption	[t]
Cresol red		8.0–10.0							
m-Cresol purple		8.5–10.5							
Thymol blue		9.0–12.0							
Brilliant yellow		7.0–9.0							
Phenol red	NA	6.5–8.5	0.1	NA	NA	NA	NA	Reflectance	[t]
Phenol red nylon		8.0–10.0							
Cresol red		8.5–10.5							
m-Cresol purple		9.0–12.0							
Thymol blue		9.0–12.0							
Brilliant yellow		7.0–9.0							

[a]Bellerby *et al.* (2002).
[b]Wong *et al.* (2005).
[c]Lau *et al.* (2006).
[d]Taboada Sotomayor *et al.* (1997).
[e]Wróblewski *et al.* (1998).
[f]Creaser *et al.* (2002).
[g]Michie *et al.* (1995).
[h]Flannery *et al.* (1997).
[i]Chan *et al.* (1998).
[j]Jin *et al.* (2001).
[k]Hulth *et al.* (2002).
[l]Niu *et al.* (2005).
[m]Schroeder *et al.* (2005).
[n]Sanchez-Barragan *et al.* (2005).
[o]Li *et al.* (2006).
[p]Vuppu *et al.* (2009).
[q]Aller and Zhu (2006).
[r]eXact® Micro 7+ pH (http://www.sensafe.com).
[s]Optical pH sensors (http://www.polestartech.com).
[t]Fiber optic pH sensor (http://www.oceanoptics.com).
NA, not available;
CI: confidence interval; RSD: relative standard deviation; 4-CP-BPB: (4-carboxyphenyl)-bromophenol blue; TBPSP: 3,4,5,6-tetrabromophenolsulfonephthalein; PoAnis/TSA: poly(omethoxyaniline) doped by *p*-toluene sulfonic acid; bpy: 2,2′-bipyridine; dhphen: 4,7-dihydroxy-1,10-phenanthroline; BNS: 6-bromo-2-naphthyl sulfate; BrN: α-bromonaphthalene; PhR: Phenol red; BCP: Bromocresol purple; BPB: Bromophenol blue; HPTS: 8-hydroxypyrene 1,3,6-trisulfonic acid trisodium salt; TAPP: *meso*-5,10,15,20-tetra-(4-allyloxyphenyl)porphyrin; MBTD: *N*-(2-methacryloxyethyl)benzo[*k*,*l*]thioxanthene-3,4-dicarboximide; DHFA: 2′,7′-dihexyl-5(6)-*N*-octadecylcarboxamidofluorescein; DHFAE: 2′,7′-dihexyl-5(6)-N-octadecyl-carboxamidofluorescein ethyl ester; $Ru(dpp)_3$: tris(4,7-diphenyl-1,10-phenanthroline)ruthenium(II); DLR: dual lifetime referencing; Mercurochrome: 2′,7′-dibromo-5′-(hydroxymercuri)fluorescein; APN: *N*-allyl-4-piperazinyl-1,8-naphthalimide; MAHPDS: 6-methacryloyl-8-hydroxy-1,3-pyrene disulfonic acid; FITC-dextran: fluorescein isothiocyanatedextran.

in situ, continuous monitoring of the analyte over a wide concentration range and are unaffected by water parameters such as color and turbidity. Yet, electrochemical devices for ion sensing may lack the required precision and suffer from interfering species (false-positive readings, explained later).

The so-called ion–selective electrodes (ISE; the pH electrode is actually an ion-selective electrode) are commercially available for most ionic species commonly present in water samples, namely ammonium, chloride, iodide, fluoride, nitrate, potassium, sodium, and many heavy metals. Amperometric measurements of a galvanic cell based on the electrical potential created across an ion-specific solid membrane due to the presence of the target ion, versus that of a reference electrode (Figure 2), allows determination of the analyte ion activity. The analyte-sensitive membrane is placed at the bottom of a small reservoir containing the (internal) reference electrode held at constant potential, and the sensor is introduced into the sampled water.

For instance, the ISE for fluoride in water contains as an analyte-selective membrane, a single LaF_3 crystal doped with EuF_2 to create defects that improve conductivity of the F^- ions within the solid. However, the calcium ISE is based on a plasticized poly(vinyl chloride) (PVC) membrane containing an organic receptor that binds and transports Ca^{2+} across the film. This transportation is responsible for the buildup of an electrical potential between the two sides of the membrane, so that the measured current is proportional to the concentration of the target ion in the aqueous medium where the ISE is immersed.

Table 3 summarizes some of the instruments, available in the market, that use ISEs for ion monitoring in water. This chapter does not aim to provide an extensive description of every commercial instrument, but to provide a general outline on the state of the art of this technology.

In situ continuous sensing of waterborne bromide, calcium, chloride, and fluoride using solid-state transducers (i.e., the inner electrolyte is replaced by a semi-solid paste), and ammonium and nitrate using PVC-coated electrodes, is provided by Nexsens ISE WQSensors (Table 4). All of them show measurement reproducibility better than 4% and are based on screw-cap replaceable sensing modules, simplifying maintenance operations. They have a 1.8-m USB connector cable for direct data collection by a computer and for freeing them from individual power supplies.

The Nico2000 ELIT ISE sensors (Table 5) are another example of commercial electrochemical sensors. The two-head configuration (reference + ISE) allows the user to replace only the electrode without changing the head. A multicomponent analysis is offered with a configuration of one reference with up to six ion sensors. With a response time of just 10 s, this company offers an impressive list of sensors for waterborne ions.

The Yellow Spring 6000 series is an example of combined multiparametric electrochemical/optical sensing modules (see below). Unlike the ISEs mentioned above, these sensor modules have their own power supply to improve the positional freedom for *in situ* monitoring. Capable of working from -5 to 50 °C, its chloride, nitrate, and ammonium sensors seem ideal for nutrient environmental monitoring. The latter two contain a PVC membrane impregnated with a specific reagent yielding a working range of 0–200 $mg\,l^{-1}$ (0.001–1 $mg\,l^{-1}$ resolution), while the chloride ISE uses a solid-state membrane that allows monitoring from 0 to 1000 $mg\,l^{-1}$ (with the same resolution as the other two).

Horiba Process & Environmental Sensor Technology (NJ, USA) has developed a multiparameter sensing probe capable of simultaneously analyzing up to 13 different parameters including a variety of ions in the temperature range of 0–55 °C. The W-20 series is a probe with high-pressure tolerance allowing measurement of nitrate, chloride, and fluoride at depths up to 100 m in rivers, lakes, or even in the open sea, accompanied by its built-in memory capacity of 1 month data logging. One of its attractive features is its global positioning system (GPS) module that allows acquisition of the location and time of each measurement for detailed three-dimensional (3D) records.

Both Analytical Technology Inc. (ATI) and Hach market sensors that rely on the change of the sample acidity to extract the analyte into the headspace, as described earlier. The ATI's A15/79 total residual chlorine sensor actually measures the concentration of gaseous iodine in an indirect method, measuring 0.01–2000 $mg\,l^{-1}$ analyte in 3 min. It uses potassium iodide and a pH 4 buffer as reagents for the hypochlorite determination in water:

$$HClO + 2KI + HCl \rightarrow I_2(g) + 2KCl + H_2O$$

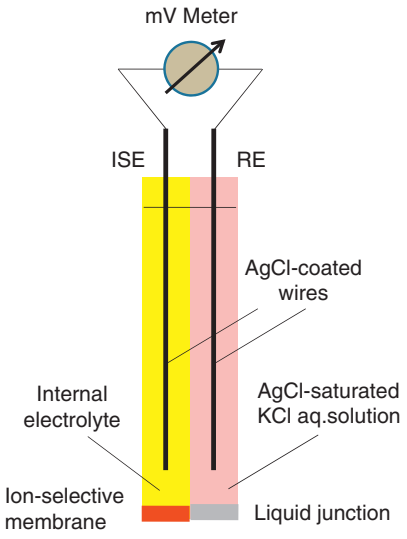

Figure 2 Typical combination ion-selective electrode.

3.10.3.2 Optical Ion Sensors

Optical sensors based on the absorption of light by the analyte ion and rugged miniature spectrometers are becoming very popular for *in situ* water monitoring due to their particular advantages compared to their electrochemical counterparts: no need of electrolyte, electrode, or membrane maintenance; sturdiness of the sensitive optical probes; absence of drift due

Table 3 Analytical data for some commercially available electrochemical sensors for waterborne ions

Ionic species	*Sensor model*	*Dynamic range (mg l^{-1})*	*Accuracy*	*Response Time (s)*	*Observations*
Ag^+, Br^-, NO_3^-, Li^+, ClO_4^-, Ca^{2+}, Na^+, K^+, NH_4^+, S^-, Cl^-, CN^-, F^-, I^-, SCN^-	AB 6000 series[a]	NA	NA	NA	Single-parameter monitoring
Br^-, Cd^{2+}, Ca^{2+}, Cl^-, Cu^{2+}, CN^-, F^-, I^-, Pb^{2+}, SO_4^{2-}, NO_3^-, K^+, Ag^+, S^{2-}	HI98184 and HI98185[b]	0.01–saturation (depending on the analyte)	NA	NA	Multiparameter monitoring
Br^-, Ca^{2+}, Cl^-, F^-, NH_4^+, NO_3^-	WQSensors[c]	See Table 4	NA	NA	Replaceable membrane, single-parameter sensors
ClO^-/Cl_2 (as total chlorine)	Q45H/62-63[d]	0–0.2; 0–2; 0–20; 0–200	0.02 mg l^{-1}	60	Polarographic gas sensor
	PCA 330 series[b]	0–5	8%	180	Multiparameter monitoring
	Chlori::lyser™[e]	0.001–2; 0.01–10	NA	120	Single-parameter monitoring
Cl_2, ClO_2, F^-	Conex® DIA[f]	0–50 (depending on the analyte)	NA	NA	Multiparameter monitoring
Cl^-, NH_4^+ and NO_3^-	YSI 6000 series[g]	0–200; 0–1000 (see text)	10%	NA	Replaceable membrane, single-parameter monitoring
F^-	CA610[h]	0.1–10	10%	<260	Single-parameter monitoring
	A15/82[d]	0–1; 0–1000	5%	90	
	IF–250[i]	0–20; 0–200; 0–2000; 0–10 000	30%	*NA*	
K^+	C–131[i]	339–3900	NA	NA	
Na^+	C–122[i]	23–2300	NA	NA	
	SODITRACE[j]	1×10^{-6}–10	10%	120	
	9245[h]	1×10^{-5}–10	5%	180	
NH_4^+	AMTAX™ [h]	0.02–5; 0.05–20; 1–100; 10–1000	<5%	<300	Gas-sensitive electrode
	Monitor FAM ammonium[j]	0.1–1000	10%	NA	Single-parameter monitoring
NH_4^+, Cl^-, CN^-, F^-, NO_3^-, NO_2^-	ES 9010[k]	0.003–1000 (depending on the analyte)	NA	600	Multiparameter monitoring
NH_4^+, Ba^{2+}, Br^-, Cd^{2+}, Ca^{2+}, Cl^-, Cu^{2+}, CN^-, F^-, I^-, Pb^{2+}, Hg^{2+}, NO_3^-, NO_2^-, ClO_4^-, K^+, Ag^+, Na^+, S^{2-}, SCN^-	ELIT[l]	See **Table 5**	10%	10	Replaceable membrane, multiparameter system
NH_4^+, NO_3^-, Cl^-	TROLL 9500[m]	0.14–14 000 N 0.35–35 500 Cl	10% N and 15% Cl	60	Multiparameter monitoring
NH_4^+, NO_3^-, K^+	Ammo::lyser™ pro[e]	0.1–1000	NA	60	Multiparameter monitoring
NO_3^-	Monitor FAM Nitrate[j]	0.1–1000	10%	NA	Single-parameter sensors
	B-343[l]	14–1400	10%	NA	
NO_3^-, Cl^-, Ca^{2+}, F^-, K^+	W-20 Series[i]	0.02–62 000 (depending on the analyte)	10%	NA	Multiparameter monitoring
SO_3^{2-}	A15/66[d]	0–20; 0–2000	0.03 mg l^{-1}	180	Polarographic gas sensor
H_2S^-, S^{2-} (as dissolved sulfide)	A15/81[d]	0–20; 0–2000	0.03 mg l^{-1}	180	Polarographic gas sensor

[a]ASTI (http://www.astisensor.com).
[b]HANNA instruments (http://www.hannainst.com).
[c]Nexsens (http://www.nexsens.com).
[d]ATI (http://www.analyticaltechnology.com).
[e]S::can (http://www.s-caNAt).
[f]Grundfos Alldos (http://www.grundfosalldos.com).
[g]YSI (http://www.ysi.com).
[h]Hach (http://www.hach.com).
[i]HORIBA (http://www.horiba.com).
[j]SWAN (http://www.swan.ch).
[k]Environnement S.A. (http://www.environnement-sa.com).
[l]NICO 2000 (http://www.nico2000.net).
[m]In-Situ Inc. (http://www.in-situ.com).
NA, not available.

Table 4 Technical details on Nexsens ISE WQsensors

Ion	*Working range (mg l^{-1})*	*Temperature range (°C)*	*Known interferents*
Br^-	0.4–79 900	0–80	I^-, Cl^-, S^{2-}, CN^-, NH_3
Ca^{2+}	0.02–40 000	0–40	Pb^{2+}, Hg^{2+}, Si^{2+}, Fe^{2+}, Cu^{2+}, Ni^{2+}, NH_3, Na^+, Li^+, $Tris^+$, K^+, Ba^{2+}, Zn^{2+}, Mg^{2+}
Cl^-	0.18–35 500	0–80	CN^-, Br^-, I^-, OH^-, S^{2-}, NH_3
F^-	0.02 to saturation	0–80	OH^-
NH_4^+	0.014–1400 (N)	0–50	Na^+, K^+
NO_3^-	0.1–14 000 (N)	0–50	ClO_4^-, I^-, ClO_3^-, F^-

Table 5 Technical data for the ELIT ion sensors

Ion	*Dynamic range (mg l^{-1})*	*Temperature range (°C)*	*Known interferents*
Ag^+	0.01–107 900	0–80	Hg^{2+}, S^{2+}
Ba^{2+}	0.5–13 700	0–50	Ca^{2+}, K^+, Na^+, Mg^{2+}, NH_4^+, Sr^{2+}
Br^-	0.4–80 000	0–80	Ag +, CN^-, I^-, S^{2-}, Cl^-
Ca^{2+}	0.02–40 000	0–50	Al^{3+}, Ba^{2+}, Fe^{2+}, Cu^{2+}, Sr^{2+}
Cd^{2+}	0.1–11 000	0–80	Ag^+, S^{2-}, Cu^{2+}, Fe^{2+}, Fe^{3+}, Hg^{2+}, Pb^{2+}
Cl^-	1–35 000	0–80	Br^-, CN^-, I^-, S^{2-}, Ag^+
ClO_4^-	0.2–99 600	0–50	Cl^-, I^-, NO_3^-, SCN^-
CN^-	0.03–260	0–80	I^-, S^{2-}, Ag^+
Cu^{2+}	0.006–64 000	0–80	Ag^+, Br^-, Cd^{2+}, Cl^-, Fe^{2+}, Hg^{2+}, S^-
F^-	0.06–2000	0–80	OH^-
Hg^{2+}	0.2–201 000	0–80	Ag^+, S^{2-}
I^-	0.06–127 000	0–80	CN^-, S^{2-}, Ag^+, $S_2O_3^{2-}$
K^+	0.4–39 000	0–50	Cs^+, NH_4^+
Na^+	0.05–20 000	0–50	Most cations
NH_4^+	0.03–9000	0–50	K^+
NO_3^-	0.3–62 000	0–50	BF_4^-, Cl^-, ClO_4^-, CN^-,I^-, NO_2^-, HCO_3
NO_2^-	0.5–460	0–50	CN^-, CH_3COO^-, F^-, Cl^-, NO_3^-, SO_4^{2-}
Pb^{2+}	0.2–20 800	0–80	Ag^+, S^{2-},Cd^{2+}, Cu^{2+}, Fe^{2+}, Fe^{3+}, Hg^{2+}
S^{2-}	0.003–32 000	0–80	Ag +, Hg^{2+}
SCN^-	1–5800	0–80	Br^-, Cl^-, I^-, Ag +, S^{2-}, $S_2O_3^{2-}$

to a reference electrode; lack of electrical interferences; and ease of miniaturization. However, they may be subject to interference due to turbidity or the presence of species other than the analyte absorbing in the same region (e.g., dissolved organic matter or ions other than the monitored ones).

For example, S::can (Austria) provides robust sensors for nitrate and nitrite monitoring by measuring the ultraviolet (UV)–visible (VIS) absorption spectrum of these ions in the water. Determinations are possible by using chemometrics, a term coined in the 1970s to design the use of statistical methods for the analysis of (instrumental) analytical chemistry data (Brereton, 2007). Registration of thousands of spectra from known samples allows training the optical sensors for recognizing the analyte pattern and quantifying it in the actual (complex) water matrices.

The multiparameter Tethys UV400 instrument (Meylan, France) also relies on spectral absorption by the sample to provide quantitative information on ammonium, nitrate, phosphate, and hydrogen sulfide. By measuring the UV light absorption at 210–220 nm, the instrument provides a working range of 0–100 mg l^{-1} for nitrate. The ammonium-detection method is based on increasing the pH of the water by the addition of sodium hydroxide to transform all dissolved NH_4^+ into gaseous NH_3, which has a distinct absorption around 200 nm. The sensor is able to measure 0–100 mg l^{-1} of ammonia free of interferents since the detection occurs in the gaseous phase. By acidifying the sample upon addition of hydrochloric acid, this device enables the extraction of gaseous H_2S from the dissolved HS^-. Phosphate determinations are made by colorimetric measurements, yielding a working range of 0–2 mg l^{-1}.

Several other instruments also rely on absorption methods for multiparameter sensing purposes. The Swan AMI Phosphate monitor (Hinwill, Switzerland) for automatic and continuous measurements of 0.01–10 mg l^{-1} phosphate in water uses the ammonium molybdate ISO 6878 colorimetric method to work for up to 6 months, with a response time of 10 min within a temperature range from − 10 to 50 °C.

Hach (Loveland, CO, USA) has developed several continuous monitoring single- and multiparameter optical chemical sensors. For instance, the MO42 Molybdate Analyzer uses colorimetric catechol chemistry detection at 420 nm to monitor molybdenum oxoanions with a limit of detection of 0.03 mg l^{-1} and a dynamic range of 0–5 mg l^{-1}. Being capable of working for up to 1 month of unattended operation, it shows readings every 2.5 min, ensuring proper monitorization. A cuprethol colorimetric method enables the APA 6000™ instrument to analyze copper (II) at 436 nm in two separate ranges, 0.05–2.0 mg l^{-1} and 1–10 mg l^{-1}. This device is also capable of 1 month of unattended operation, and it measures readings every 4 min, yielding results with a resolution of 0.001 mg l^{-1}. The same company also provides several solutions to monitor water hardness (magnesium and calcium), using both the APA 6000™ low-range hardness analyzer and the SP510 instruments, monitoring in the working range of 0.05–10 mg l^{-1} (as $CaCO_3$). As in other instruments that use optical methods for the detection of nitrate and nitrite, the Hach Nitratax™ monitor takes advantage of the molecular N–O bond UV light absorption to obtain its concentration, using a second beam of light to eliminate interference from turbidity and dissolved organic matter. This reagent-free UV-absorption technique gives a dynamic range from 0.1 to 100 mg l^{-1} (as N) with a resolution of 0.1 mg l^{-1}.

Phosphax™ is the Hach instrument for phosphate optical detection. With a self-cleaning membrane, it is capable of detecting from 0.05 to 50 mg l^{-1} (in phosphorous) with a 5-min response time and 3 months of unattended operation. Table 6 lists some of the instruments that use optical methods for continuous detection of ionic species in water.

When considering optical monitoring of waterborne ions, there are very few instruments capable of *in situ* continuous sensing (basically nitrates and phosphates). However, there are several portable devices capable of detecting numerous ions in water samples by optical methods that require human intervention for sampling, conditioning, and testing operations. For instance, a portable photometer, such as the Hach DR 2700™, provides fast results with its multiwavelength capability. It is able to detect an impressive number of ionic species with adequate limits of detection.

Test strips are also a good example of widespread simple optical dosimeters as the changes in color of an immobilized specific reagent in the presence of the target analyte yield direct quantification. Even though this type of sensing

Table 6 Some of the optical instruments commercially available for ionic species monitoring

Ionic species	*Sensor model*	*Dynamic range* (*mg* l^{-1})	*Accuracy*	*Response time* (s)	*Remarks*
Cl_2, ClO_2	AMI CODES-II CC[a]	0–1; 1–3; 3–5	0.01; 0.06; 0.2 mg l^{-1}	120	DPD method
	CL17[b]	0.035–5	5%	<150	DPD method
Cu^{2+}	APA 6000™[b]	0.05–2; 1–10	5%	<240	Colorimetric cuprethol chemistry
Mo^{6+}	MO42[b]	0.03–5	5%	<150	Colorimetric catechol chemistry
NO_3^-	ISUS V3[c]	0.007–28	0.028 mg l^{-1}	NA	UV absorption
	nitro::lyser™[d]	0–70	3%	NA	UV–VIS spectrometry over the total range, multiparameter probe
	multi::lyser™[d]	0–70	3%	NA	
NO_3^-, NO_2^-	spectro::lyser™[d]	From 0 to 50 (N) (depending on the analyst)	3%	NA	
	TPNA–300[e]	0–2 (N)	NA	3600	Measures total nitrogen through alkaline potassium peroxodisulfate UV oxidation–UV absorption method
	YSI 9600[f]	0.025–10	5%	NA	Cadmium reduction–diazotization colorimetric method
	NITRATAX™[b]	0.1–100	5%	60	UV absorption
PO_4^{3-}	PHOSPHAX™[b]	0.05–15; 1–50	2%	<300	Colorimetric molybdovanadate chemistry
	Series 5000[b]	0.2–50	5%	660	
	TPNA–300[e]	0–0.5 (P)	NA	3600	Measures total phosphorus by potassium peroxodisulfate UV oxidation–molybdenum blue absorption method
	Monitor AMI Phosphate[a]	0.01–10	NA	600	Ammonium molybdate colorimetric method
NH_4^+, HS^-, S^{2-}, NO_3^-,NO_2^-, PO_4^{3-}	UV400[g]	From 0 to 79 (depending on the analyse)	NA	5	UV absorption and colorimetric Multiparameter instrument

[a]SWAN (http://www.swan.ch).
[b]HACH (http://www.hach.com).
[c]Satlantic (http://www.satlantic.com).
[d]s::can (http://www.s-canat).
[e]HORIBA (http://www.horiba.com).
[f]YSI (http://www.ysi.com).
[g]TETHYS Instruments (http://www.tethys-instruments.com).
NA, not available.

Table 7 Examples of the test strips for ion analysis offered by three manufacturers

Ion	*Dynamic range*	*Manufacturer*	*Ion*	*Dynamic range*	*Manufacturer*
Al^{3+}	10–250 mg l^{-1}	Merck	Mo^{6+}	5–250 mg l^{-1}	Merck
	0.01–0.25 mg l^{-1}	Jenway		0.3–18 mg l^{-1}	Jenway
NH_4^+	10–400 mg l^{-1} N	Merck	Hg^{2+}	50–1000 μg l^{-1}	ITS
	1–50 mg l^{-1} N	Jenway		2–80 μg l^{-1}	
$As^{3+/5+}$	0.1–3 mg l^{-1}	Merck	Ni^{2+}	10–500 mg l^{-1}	Merck
	0.005–0.5 mg l^{-1}				
Ca^{2+}	10–100 mg l^{-1}	Merck	NO_3^-	10–500 mg l^{-1}	Merck
Cl^-	0.5–20 mg l^{-1}	Merck		1–30 mg l^{-1} N	Jenway
	25–500 mg l^{-1}				
	50–500 mg l^{-1}	ITS		0.5–50 mg l^{-1}	ITS
$Cr^{3+/6+}$	0.02–2 mg l^{-1}	Jenway	NO_2^-	100–3000 mg l^{-1}	Merck
	0.1–50 mg l^{-1}	ITS		2–80 mg l^{-1}	
CrO_4^{2-}	3–100 mg l^{-1}	Merck		0.01–0.5 mg l^{-1} N	Jenway
Co^{2+}	10–1000 mg l^{-1}	Merck		0.15–10 mg l^{-1}	ITS
$Cu^{+/2+}$	10–300 mg l^{-1}	Merck	PO_4^{3-}	10–500 mg l^{-1}	Merck
	0.5–5 mg l^{-1}	Jenway; ITS		0.05–4 mg l^{-1} PO_4	Jenway
	0.05–2 mg l^{-1}	ITS	K^+	250–1500 mg l^{-1}	Merck
Ag^+	0.5–10 g l^{-1}	Merck		0.5–12 mg l^{-1}	Jenway
	0.05–1 mg l^{-1}	ITS	SO_4^{2-}	200–1600 mg l^{-1}	Merck
	5–100 μg l^{-1}			2–100 mg l^{-1} SO_4	Jenway
$Fe^{2+/3+}$	3–500 mg l^{-1}	Merck	SO_3^{2-}	10–400 mg l^{-1}	Merck
	0.1–3 mg l^{-1}	Jenway		0.05–4 mg l^{-1} SO_3	Jenway
	0.005–0.3 mg l^{-1}	ITS	Sn^{2+}	10–200 mg l^{-1}	Merck
	0.02–5 mg l^{-1}				
	0.3–50 mg l^{-1}				
Pb^{2+}	20–500 mg l^{-1}	Merck	Zn^{2+}	10–250 mg l^{-1}	Merck
	3–600 μg l^{-1} (with photometer detection)	ITS		0.02–1 mg l^{-1} Zn	Jenway
F^-	0.02–1.5 mg l^{-1}	Jenway		2–100 mg l^{-1}	ITS
Mn^{2+}	2–100 mg l^{-1}	Merck			
	0.05–4 mg l^{-1}	Jenway			
	0.02–1.6 mg l^{-1}	ITS			

mechanism does not constitute a true sensor (see Section 3.10.1), colorimetric test strips are very much in use for *in situ* semi-quantitative quick detection of ionic species in water samples. Several companies offer such convenient strips: for instance, the Merckoquant® strips (Merck, Germany) allow visual detection and quantitation of numerous ions in aqueous media. Some test-strip methods require the use of a portable or handheld reflectophotometer to improve accuracy of analyte determination and reproducibility. Cases in point are the Jenway environmental test kits (Belgium) or Industrial Test Systems Inc. strips with their 3 μg l^{-1} lead-detection test using the Hach LeadTrak Pocket Colorimeter II providing limits of detection lower than the US EPA requirement (15 μg l^{-1}). Table 7 summarizes the ions covered by the test strips offered by the above-mentioned manufacturers.

3.10.4 Sensors for Dissolved Carbon Dioxide

Carbon dioxide is the major end product of organic carbon degradation in almost all marine environments. Fluctuations of the CO_2 level are related to the net ecosystem metabolism. Four parameters define the marine CO_2 system: pH, pCO_2, dissolved inorganic carbon, and total alkalinity. The solubility of CO_2 in the water is about 28 times that of other hydrophobic gases such as O_2 or N_2. One of the most popular methods for carbon dioxide determination in the gas phase is infrared (IR) spectrometry. For measurements in aqueous solutions, the Severinghaus pCO_2 electrode is the most common potentiometric sensor.

3.10.4.1 IR Spectrometry

Carbon dioxide can be analyzed by IR spectrometry because of its strong stretching bands at 2350 and 650 cm^{-1}. By measuring the intensity of these bands, CO_2 is quantified. This feature may be used to determine the carbon dioxide generated after acidification of aqueous samples and to calculate in this manner the total inorganic carbon (TIC) of the water.

Total inorganic carbon (also called dissolved inorganic carbon (DIC)) includes all the carbon-containing inorganic species present in solution, namely, CO_2, H_2CO_3, HCO_3^-, and CO_3^{2-}. By acidification of the water sample, the acid–base equilibria of these species are driven to CO_2 production. Nevertheless, the application of IR spectrometry to TIC determination is limited due to the strong IR absorption of water as well as the long optical path lengths required for analyses in the gas phase.

3.10.4.2 The pCO_2 Electrode

The equilibrium between the gas phase and water obeys Henry's law, which states that, for an ideally diluted solution, the gas vapor pressure of a volatile solute is proportional to its mole fraction in the aqueous solution. For surface waters (i.e., at atmospheric pressure), Henry's law can be simplified to Equation (7):

$$[CO_2] = K_H pCO_2 \tag{7}$$

where K_H represents the so-called Henry's constant and pCO_2 is the partial pressure of this gas. The pCO_2 values can be determined by using an electrode such as the Severinghaus one, based on the detection of pH changes in an internal HCO_3^- aqueous solution caused by the incoming CO_2. This solution is entrapped between a glass pH electrode and a hydrophobic gas-permeable membrane. The latter permits the flow of small, uncharged (gas) molecules such as CO_2, but prevents the entrance of charged molecules (hydrogen ions, cations, anions, etc.). In natural aquatic environments, pCO_2 varies widely between $0.1–10^{-4}$ (e.g., coastal ocean surface waters) and almost 200 atm (nearshore sediments).

The Severinghaus electrode presents important drawbacks: interferences caused by basic or acidic gases, slow response time, and effects of osmotic pressure caused by variable salt conditions in the sample and in the inner electrolyte.

3.10.4.3 Optical pCO_2 Sensors

Like pH sensors, optical pCO_2 sensors (optodes) for water are an alternative in specific applications. While electrochemical sensors employ a glass pH electrode to monitor pH changes, optical devices rely on immobilized pH-sensitive indicator dyes (see Section 3.10.2.2) to accomplish the pH transduction process within the internal electrolyte.

As in electrochemical pCO_2 sensors, the acidity of the internal solution at equilibrium depends on the concentration of carbonic acid produced upon hydration of the permeated CO_2, which in turn is proportional to the partial pressure of the analyte in the sample. Based on the pH changes produced by CO_2 diffusion through a gas-permeable membrane in an internal reservoir of hydrogen carbonate buffer, YSI Life Sciences (Yellow Springs, OH, USA) commercialized the first optical pCO_2 sensor. The latter uses the pH-sensitive fluorescent dye hydroxypyrene trisulfonic acid (HPTS, pyranine) and ratiometric fluorescent measurements (measuring the green emission upon successive excitation at two wavelengths) to determine the dissolved CO_2 concentration.

Mills *et al.* introduced a new scheme to design optical pCO_2 sensors. They incorporated a pH-sensitive dye into a hydrophobic polymer membrane (e.g., cellulose acetate butyrate) and replaced the hydrogen carbonate internal buffer by a lipophilic hydrated quaternary ammonium hydroxide. Depending on the pK_a and concentration of the indicator dye used, such sensors allow quantification of trace levels of CO_2 and show a fast response. However, the membranes tend to fog after prolonged immersion in water and, sometimes, are prone to dye leaching. A thorough description of the different types of optical sensors for CO_2 measurements can be found in the review by Mills and Eaton (2000).

Orellana and co-workers (1992) patented a CO_2 sensing mechanism based on luminescent Ru(II) polyazaheterocyclic complexes immobilized in hydrogels, that undergo irreversible proton transfer in their excited state from various Brönsted acids. The polymer-supported indicator dye is separated from the sample by a thin silicone membrane. Permeation of the CO_2 into the gel phase modifies the concentration of the internal buffer species (with different proton transfer ability, e.g., hydrogen phthalate and phthalic acid) changing the H^+-transfer quenching of the luminescent indicator dye (Figure 3). Both emission intensity and luminescence-lifetime-based interrogation can be used to fabricate the sensor using the same instrumentation than the one developed recently for dissolved oxygen sensing (see Section 3.10.5). This version is used by Optosen™ Interlab IE (Madrid, Spain) in the luminescent dissolved O_2/CO_2 monitors that they market.

Ru(II) polypyridyl complexes can also be used in combination with colorimetric indicator dyes to manufacture luminescent sensors based on Förster resonance energy transfer (FRET) from the photoexcited metal dye (donor) to the co-immobilized colorimetric indicator (acceptor). Permeation of CO_2 into the gel phase containing the two dyes lowers its pH leading to a color change. The spectral shift of the acceptor provokes a variation in the FRET efficiency with concomitant change in the emission lifetime of the donor. This principle forms the basis of the PreSens (Regensburg, Germany) dissolved CO_2 monitoring system.

3.10.4.4 Miscellaneous pCO_2 Sensors

Martek Instruments (Raleigh, NC, USA) offers a dissolved carbon dioxide analyzer based on conductivity measurements carried out before and after degassing the water sample. The conductivity differences are due to the carbonate and bicarbonate species that carbon dioxide forms when it is in solution.

Table 8 provides a summary of the prototype and commercial sensors for dissolved CO_2 measurements.

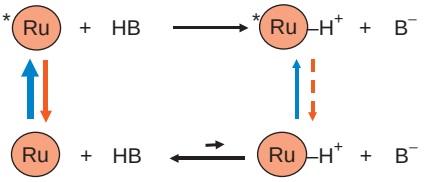

Figure 3 Working principle of the luminescent CO_2 sensor based on photoinduced proton transfer to excited Ru(II) polypyridyls (Orellana *et al.*, 2000). The ground state complex is completely non-protonated ($pK_a = -1.9$); however, its basicity increases more than 10^6-fold in its excited state due to the high-acceptor character (low-lying π^* orbital) of the pyrazine ligands. Therefore, it undergoes efficient (irreversible) proton transfer from suitable Brönsted acids present in the reservoir indicator phase (phosphate, hydrogen phthalate, acetic acid, H_3O^+, etc). The incoming CO_2 hydrolyzes and reversibly increases the HB/B^- ratio leading to strong luminescence quenching of the indicator dye.

Table 8 Some prototype and commercial sensors for carbon dioxide determination in aqueous solution

Dynamic range (ppm)	*Limit of detection (LOD) (ppm)*	*Precision*	*Response time*	*Recovery time*	*Temperature(s) tested (°C)*	*Interferences*	*Lifetime*	*Transduction principle*	*References*
30–180	NA	NA	5–120 s	NA	NA	NA	NA	Electrochemical	[a]
200–1000	NA	±1 ppm	<130 min	NA	5–23	Temperature	4 months	Fluorescence	[b]
NA	NA	NA	42.6 s	88.8 s	10–30	HCl	NA	Fluorescence	[c]
0.044–880	0.044	NA	<126 s	240 s	25	Not tested	NA	Absorption	[d]
0.17–880	NA	5.8% (relative standard deviation, RSD)	16 s	30 s	25	NA	NA	Fluorescence	[e]
0.18–440	NA	NA	<1 min	>6 min	0–40	H_2S, CH_3COOH, temperature	NA	Fluorescence	[f]
NA	0.33	NA	3 min	10 min	NA	NA	4 weeks	Fluorescence	[g]
0–900	0.50	<2%	7 min	12 min	5–35	Temperature	NA	Fluorescence	[h]
Up to 50% (832 ppm) (at 20°C and 1 bar)	NA	<2.0%	1 min	NA	20	Oxygen (>21%), temperature	NA	Luminescence	[i]
0.3–4.4	0.3	NA	1–2 min	NA	NA	NA	12 months	Fluorescence	[j]
0.05–7 hPa (0.07–10 ppm)	0.04 hPa (0.06 ppm)	NA	<30 s	<40 s	25–63	H_2S	2 months	Luminescence	[k]
15–1500	15	±10%	<120 s	NA	0–60	NA	NA	Electrochemical	[l]
4.4–400	NA	±2%	NA	NA	0–50	NO_2^-, HSO_3^-, HOAc, HCOOH	NA	Electrochemical	[m]
1–25% (16.65–416.22 ppm) (at 20 °C and 1 bar)	NA	NA	<7 min	NA	20–40	NA	NA	Fluorescence	[n]
1–25% (16.65–416.22 ppm) (at 20 °C and 1 bar)	NA	±0.06%	<3 min	NA	15–45	Salinity, acids, SO_2, HCl	6 months	Luminescence	[o]
0–10	NA	±2.0 ppb	NA	NA	0–100	NA	Analyzer: 5 years	Conductivity	[p]

[a]Wiegran *et al.* (1999).
[b]Tabacco *et al.* (1999) and Walt *et al.* (2000).
[c]Amao and Nakamura (2005).
[d]Oter *et al.* (2006).
[e]Ertekin and Alp (2006).
[f]Müller and Hauser (1996).
[g]Burke *et al.* (2006).
[h]Wolfbeis *et al.* (1998).
[i]Orellana *et al.* (1992) and Interlab Optosen™ (http://www.interlab.es).
[j]Nivens *et al.* (2002).
[k]Neurauter *et al.* (2000).
[l]InPro®5000 Mettler Toledo (http://www.mtpro.com).
[m]Orion carbon dioxide electrode (http://www.thermo.com).
[n]YSI 8500 (http://www.ysilifesciences.com).
[o]Carbon dioxide sensor (http://www.presens.de).
[p]Martek Dissolved Carbon Dioxide Analyzer (http://www.martekinstruments.com).
NA, not available.

3.10.5 Dissolved Oxygen Sensors

Together with pH, dissolved molecular oxygen is one of the main analytes to be monitored in water. Oxygen levels in water are critical to determine the health of stream, river, and lake ecosystems. Efficient operation of wastewater-treatment plants requires continuous monitoring of the O_2 concentration for aeration, activated sludge, and nutrient-removal control. Tight corrosion control (e.g., nuclear power plants) requires sensing of waterborne O_2 at ppb levels. Moreover, O_2 sensors are also used as transducers for monitoring other water-quality parameters such as biological oxygen demand (BOD), chemical oxygen demand (COD), total organic carbon (TOC), etc. (see Sections 3.10.8 and 3.10.9).

The first dissolved oxygen determination was performed by L. H. Winkler in 1888 using a colorimetric method based on a titration of oxygen with thiosulfate ($S_2O_3^{2-}$) and iodine (I_2). The amount of the dissolved oxygen is proportional to the generated tetrathionate ($S_4O_6^{2-}$), which is determined by reduction of I_2 to iodide (I^-). In spite of being difficult to use for online sensing purposes, a 100 years later, this is still employed as a reference method for calibration of electrodes. Automatic measurement of dissolved oxygen based on potentiometric determination of the produced I^- has also been developed.

3.10.5.1 Electrochemical Oxygen Sensors

In the mid-twentieth century, electrochemical methods gained importance due to their fast response, possibility of *in situ* operation, and analyte nondestructive character, either in an amperometric (voltage applied or intensity of current measured) or potentiometric (intensity applied and voltage measured) mode. The DOC is proportional to the intensity or voltage measured respectively. The cumbersome, dangerous, dropping mercury electrodes gave way to amperometric sensors with solid electrodes covered with gas-permeable membranes and which were capable of being miniaturized.

The so-called amperometric 'Clark electrode' has probably been the most used O_2 sensor so far, and has been the basis of the majority of commercial electrochemical sensors sold till date (see Table 9). In a Clark electrode, oxygen is reduced on a platinum cathode covered with an oxygen-permeable membrane:

$$O_2 + 4e^- + 2H_2O \rightarrow 4OH^-$$

Oxidation of silver metal occurs at the anode with formation of silver chloride from the chloride ions dissolved in the inner electrolyte solution:

$$Ag + Cl^- \rightarrow AgCl + e^-$$

The electrochemical cell has to be polarized at about 800 mV to ensure linearity between the oxygen consumed at the cathode and the measured current. The electrode destroys the oxygen molecules, thereby requiring a minimum water flow in order to maintain equilibrium at both sides of the gas-permeable membrane. Three problems of the Clark electrode have been identified in continuous operation mode: (1) buildup of an impermeable layer of AgCl at the active anode surface that may lead to a drift in the sensor readings and eventually to failure; (2) production of OH^- ions at the cathode moves the potential of the inner electrolyte to negative values leading to a zero shift; and (3) Cl^- ions in the electrolyte eventually become depleted. These problems are normally corrected by the periodical maintenance operations of polishing the anode and replenishing the electrolyte. At the same time, the gas-permeable layer is also cleaned or changed in order to prevent algal biofouling. Moreover, there is a need to establish a polarization of the electrochemical cell, and therefore the Clark electrode needs about 10 min before the first measurement can be obtained. This warm-up time is dependent on the sensor geometry and size.

The Clark electrode readings are indeed a function of the O_2 partial pressure in the water. According to Henry's law, the O_2 depends on the water temperature and salinity, and on the atmospheric pressure (at 20 °C and ambient pressure of 1013 mbar, air-saturated water contains about 9 mg l^{-1} of O_2). Therefore, appropriate corrections for these parameters must always be applied in all sensors.

Hydrogen sulfide, a by-product of the anaerobic metabolism of bacteria (e.g., on decaying organic matter), produces the most prominent interference on O_2 measurements using the Clark electrode. Once it permeates the electrode membrane, H_2S is converted into sulfide ion at the alkaline pH of the inner electrolyte. S^{2-} reacts at the silver anode with formation of a stable precipitate of Ag_2S, which passivates the electrode that eventually stops working.

A particular amperometric system is the galvanic cell, where a spontaneous O_2 reduction at the (platinum or other noble metal) cathode take places combined with simultaneous oxidation of a readily oxidizable sacrificial anode (e.g., lead or zinc)

$$O_2 + 4e^- + 2H_2O \rightarrow 4OH^-$$

$$Zn \rightarrow Zn^{2+} + 2e^-$$

The formed $Zn(OH)_2$ turns into zinc oxide flakes (or PbO in case of a lead anode) that, unlike the AgCl of the Clark electrode, detach from the anode surface and avoid the electrode drift in long-term continuous monitoring. The polarization needed to reduce oxygen ($\sim$800 mV) is provided by the dissimilar metals of the cathode and anode (i.e., no need of external voltage application). The galvanic O_2 sensor may be regarded as a corrosion cell, where the corrosion rate is determined by the rate of oxygen consumed at the cathode. In spite of their intrinsically limited operational lifetime (typically 5 years before having to change the anode), it overcomes some of the drawbacks of the amperometric Clark electrode (neither warm-up waiting, nor electrolyte replenishment and anode servicing are required). While the galvanic cell is less sensitive to the presence of H_2S, ammonia and high levels of dissolved CO_2 produce stronger interference than in the case of the Clark electrode.

Table 9 Some commercial sensors for waterborne molecular oxygen

Transduction principle	*Model*	*Dynamic range (mg l^{-1})*	*Precision*	*LOD*	*Response time (s)*	*Temperature range (°C)*
Electrochemical/ Clark cell	DO100[a]	0–20	0.2 ppm	0.1 ppm	900	0–55
Luminescence quenching	Oxi::lyser™[b]	0–25	1%	0.01 ppm	NA	0–50
Luminescence quenching	ROX® Optical Dissolved Oxygen Sensor[c]	0–20	0.1 ppm	0.01 ppm	NA	NA
Electrochemical/ galvanic cell	Model Q45D[d]	0–40	0.2%	0.05%	NA	−20–60
Luminescence quenching	FDO® 700 IQ[e]	0–20	0.01%	NA	<150	−5–50
Electrochemical/ galvanic cell	TriOxmatic®[e]	0–60	0.1%	NA	180	0–60
Electrochemical/ galvanic cell	DC 300[f]	0–20	1.5%	0.01 ppm	NA	0–50
Luminescence quenching	ORBISPHERE G1100[g]	0–20	±2 ppb	0.6 ppb	<30	−5–50
Electrochemical/ galvanic cell	ORBISPHERE A1100[g]	0.05–2000	±1%	0.1 ppb	30	−5–60
Electrochemical/ galvanic cell	Model 9438[h]	0–20	±5%	NA	NA	−20–55
Electrochemical/ Clark cell	HI 9142[i]	0–19.9	±1.5%	0.1 ppm	NA	0–50
Luminescence quenching	ODOT[j]	0–20	±1%	0.01 ppm	<60	−10–60
Electrochemical/ Clark cell	COS21D-A[k]	0.001–20	±1%	1 ppb	<60	−5–100
Electrochemical/ Clark cell	OPTISENS AAS 2000[l]	0–20	±1%	NA	NA	0–50
Luminescence quenching	RDO® PRO[m]	0–20	±0.2%	0.01 ppm	NA	0–50
Luminescence quenching	OPTOSEN™[n]	0–40	±0.2%	0.01 ppm	NA	0–60
Luminescence quenching	LDO® Dissolved Oxygen Probe[g]	0–20	±0.1 ppm	0.01 ppm	60	0–50
Luminescence quenching	PSt3[o]	0–45	±0.4%	0.015 ppm	NA	0–50
Luminescence quenching	PSt6[o]	0–1.8	±3%	0.001 ppm	NA	0–50

[a]Stevens Water Monitoring Systems Inc. (http://www.stevenswater.com).
[b]S::can Messtechnik GmbH (http://www.s-caNAt).
[c]YSI Environmental (http://www.ysi.com).
[d]Analytical Technology Inc. (http://analyticaltechnology.com).
[e]WTW GmbH (http://www.wtw.com).
[f]OAKTON Instruments (http://www.4oakton.com).
[g]HACH Company (http://www.hach.com)
[h]ABB Inc. (http://www.abb.com).
[i]HANNA Instruments Inc. (http://www.hannainst.com).
[j]Neotek-Ponsel (http://www.neotek-ponsel.com).
[k]Endress + Hauser Inc. (http://www.endress.com).
[l]KROHNE Messtechnik GmbH & Co. (http://www.krohne.com).
[m]In-Situ Inc. (http://www.in-situ.com).
[n]Interlab IE (http://www.interlab.es).
[o]PreSens Precision Sensing GmbH (http://www.presens.de).
NA, not available.

Although concentrations of oxygen are generally measured *in situ* amperometrically, potentiometry offers an alternative way of O_2 sensing. Using the latter method, no analyte is consumed during the measurement and, at low oxygen concentrations, the logarithmic sensitivity of potentiometric sensors becomes an advantage over the linear sensitivity of amperometric sensors. Potentiometric oxygen sensors were initially developed to measure in the gas phase at high temperature; however, novel potentiometric sensors for determination of dissolved oxygen at ambient temperatures have been manufactured using transition metals (cobalt, zinc, and platinum) or metal oxides (ruthenium oxide, tungsten oxide, and iridium oxide) electrodes.

3.10.5.2 Optical Oxygen Sensors

After the original Winkler method (mentioned earlier), optical methods for measuring O_2 levels in water have also been developed. For instance, the absorption at 620 nm of indigo carmine has been employed to determine 1–8 mg l^{-1} of dissolved oxygen. This method was an improvement on the 1925 method by Efimoff that employed an indigo carmine solution, glucose as reducing agent, and potassium carbonate as pH buffer. Further modification of this procedure also led to the detection of ppb levels of O_2 in water. However, colorimetric methods require sample pretreatment, which makes their online use difficult.

When H. Kaustsky discovered in 1939 the luminescence quenching of organic molecules by dissolved oxygen, he was not aware that this opened an extraordinary door to the sensor community. Bimolecular dynamic deactivation of the electronic excited state does not consume the analyte and depends on the quencher concentration (O_2 in this particular case). It is observed as a reduction on both the luminescence intensity and lifetime of the indicator dye according to the Stern–Volmer equation

$$\frac{I_0}{I} = \frac{\Phi_0}{\Phi} = \frac{\tau_0}{\tau} = 1 + K_{SV}[O_2] = 1 + k_q\tau_0[O_2] \qquad (8)$$

where I, Φ, and τ represent the luminescence intensity, quantum yield, and lifetime of the indicator dye, respectively (the subscript 0 means in the absence of O_2), and K_{SV} is the so-called Stern–Volmer constant. The latter is equivalent to the product of the bimolecular rate constant of the quenching reaction (k_q) and the lifetime of the luminophore in the absence of O_2 (τ_0). The linearity of the Stern–Volmer law is normally lost when the luminescent indicator dye is immobilized into a polymer support for manufacturing the actual oxygen sensor by usually attaching the luminescent film at the distal end of an optical fiber (**Figure 4**).

Therefore, oxygen optical sensors can be based on luminescence intensity or lifetime changes as a function of the analyte level. Luminescence-based O_2 sensors offer advantages over electrochemical devices including ease of miniaturization, lack of analyte consumption, faster response, robustness, and insensitivity to interfering agents (e.g., H_2S, CO_2, or NH_3). The low maintenance, extended operational lifetime, and reliability of fiber-optic oxygen sensors based on transition metal (Ru, Pd, Pt, and Ir) luminescent complexes with polyazaheterocyclic chelating ligands (bipyridines and phenanthrolines, porphyrins, etc.) are so noticeable that every major manufacturer of environmental monitors is currently offering at least one model for *in situ* dissolved O_2 measurements in water (see **Table 9**), rapidly phasing out the amperometric Clark electrode.

The appropriate selection of a luminescent dye with a long excited-state lifetime and a supporting polymer material with a high O_2 permeability are key issues in the design of the ideal oxygen optical sensor. In this way, materials such as fluorinated polymers, polystyrene, aerogels, organically modified silicates (ORMOSILs), or polydimethylsiloxane (silicone) have

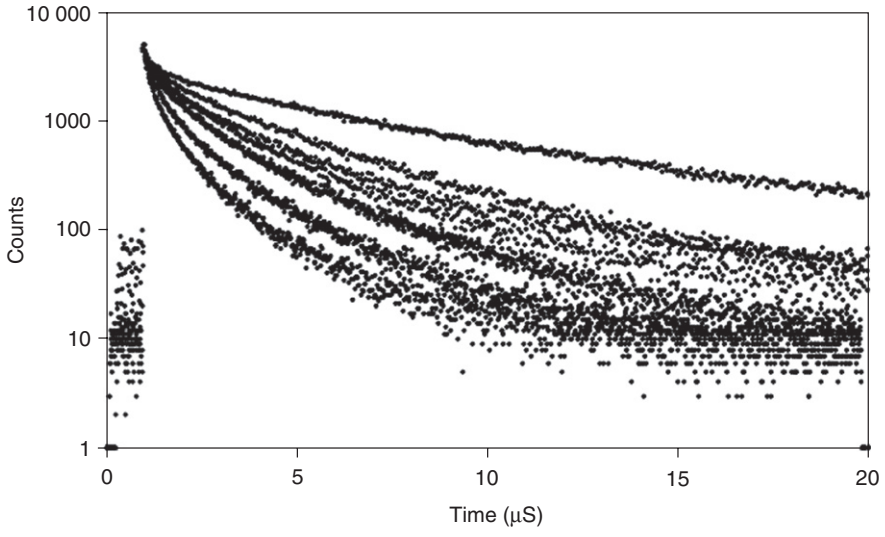

Figure 4 Luminescence decay profiles upon pulsed excitation of the O_2 indicator dye tris(4,7-diphenyl-1,10-phenanthroline)ruthenium(II) dichloride embedded in a silicone film, for different O_2 concentrations in water (from top to bottom: 0, 0.4, 0.8, 1.2, 1.6, 4.0, and 8.0 mg l^{-1}).

all been used with the aim of finding the ideal matrix for each particular application. Most of the sensing layers are microheterogeneous materials formed by the base polymer plus fillers, cross-linkers, plasticizers, etc. These components may play different roles such as reinforcement, providing dye compatibility, increasing flexibility or resistance, etc.

One of the most prominent advantages of fiber-optic oxygen sensors is the ease of miniaturization at affordable cost. Therefore, micro-optical sensors have made possible *in situ* monitoring of aquatic environments in confined spaces such as marine sediments, microbial mats, lichens, biofilms, etc.

Both electrochemical and optical sensors are subject to formation of biofilm over the luminescent sensing layer, or the electrode membrane is a critical component of continuous dissolved oxygen monitoring in high biofouling environment (wastewater-treatment plants, highly eutrophized rivers or lakes, tropical ocean bays, etc.). Vendors have developed different methods to avoid such deposits and prolong the operational lifetime of the sensors. Thus, antifouling materials (YSI Inc., Yellow Spring, OH, USA), pressurized air systems (Analytical Technology Inc., Collegeville, PA, USA), ultrasounds (WTW GmbH, Weilheim, Germany), integrated spray cleaning nozzles (KROHNE Messtechnik GmbH, Duisburg, Germany), and automatic mechanical wiping (HACH Co., Loveland, CO, USA), to name a few, are useful commercially available strategies to keep sensor biofouling at bay.

3.10.6 Sensors for Waterborne Ozone

Ozone (O_3) is a strong oxidizing gas with various industrial applications spanning from water treatment to microelectronics to pharmaceuticals. The needs of each industry in terms of concentration is very different and ranges from the high levels for water treatment, where ozone is used for purification and disinfection purposes on highly absorbing water media, to the residual ppb levels that can be found in cooling water reservoirs of the pharmaceutical or microelectronics factories. Therefore, the monitoring needs for process control and possible interferences are broadly different. For example, the O_3 concentration in wastewater treatment should be monitored carefully to keep it at the appropriate concentration that leads to effective water disinfection but minimizes the dangerous bromate ion formation from bromide.

Similar to O_2 (see Section 3.10.5), continuous monitoring of ozone can be performed by two main methods: electrochemical and optical sensing. The former is based on the electrochemical reduction of ozone over the sensor electrode. The redox method has a few disadvantages in that it is a nonspecific reduction process wherein chlorine or other oxidizing gases present in the sample can interfere with the O_3 measurements. To resolve this, several approaches have been proposed. New electrochemical amperometric ozone sensors have a membrane through which ozone diffuses and reaches the electrode. The presence of this selective membrane avoids major interference from other species but introduces a delay in the analysis and increases the equipment cost. Ozone monitoring in waters with high concentration of particulates or salts pose additional maintenance challenges to avoid membrane obstruction, with consequent increase in operational costs. A more elaborate system is the DOM-1 monitor from Eco Sensors, Inc. (Santa Fe, NM, USA). It includes a stripping chamber to extract O_3 from the liquid phase for analyzing it electrochemically in the gas phase. Apparently, the stripping separation method reduces the response time of the equipment considerably.

As far as optical methods are concerned, O_3 has been traditionally been measured by colorimetry after reaction with indigo derivatives:

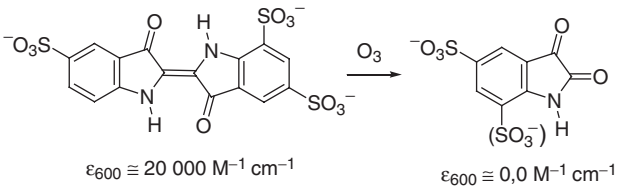

$\varepsilon_{600} \cong 20\,000\ M^{-1}\,cm^{-1}$ $\varepsilon_{600} \cong 0{,}0\ M^{-1}\,cm^{-1}$

For instance, CHEMetrics ozone dosimeter (Calverton, VA, USA) employs indigo trisulfonate. This dye reacts instantly and quantitatively with ozone, bleaching its blue color in direct proportion to the amount of ozone present. Malonic acid is included in the formulation to prevent interference for up to $3\ mg\,l^{-1}$ of waterborne chlorine.

Ozone displays a strong absorption band centered at 253.7 nm in the UV region, with an absorption cross section of $1.141 \times 10^{-17}\ cm^2$. In fact, such a strong absorption band has been in use for quite some time for O_3 measurements in the gas phase. Recently, companies such as Horiba Advanced Techno (Northampton, UK), S::can Messtechnik GmbH (Wien, Austria), and IN USA Inc. (Norwood, MA, USA) have developed new optical O_3 sensors for water analysis. In some cases (e.g., the Horiba OZ-96 sensor), the system designed for ozone monitoring in clean waters is similar to that used during the manufacturing processes of the semiconductor industry where no absorbing interferent species influence the measurements. This is not the case in the treatment of wastewater with large amounts of suspended solids and organic matter that obstructs the optical measurements. Nevertheless, some recently results from S::can Messtechnik with its Spectro::lyser™ monitor show excellent agreement between the electrochemical and optical determination of ozone concentration in wastewater (**Figure 5**). Such an accuracy in the O_3 level monitoring with an optical sensor in a complex absorbing matrix can be obtained, thanks to an elaborate data treatment using advanced chemometrics tools.

A summary of representative waterborne O_3 sensors can be found in **Table 10**.

3.10.7 Sensors for Waterborne Hydrocarbons

Hydrocarbon-in-water sensing can be divided into two applications with very different requirements and detection levels. Thus, the petrochemical industry has traditionally used sensors for detecting oil spills which have high levels of hydrocarbons in water and, very often, a very large monitoring area. To this

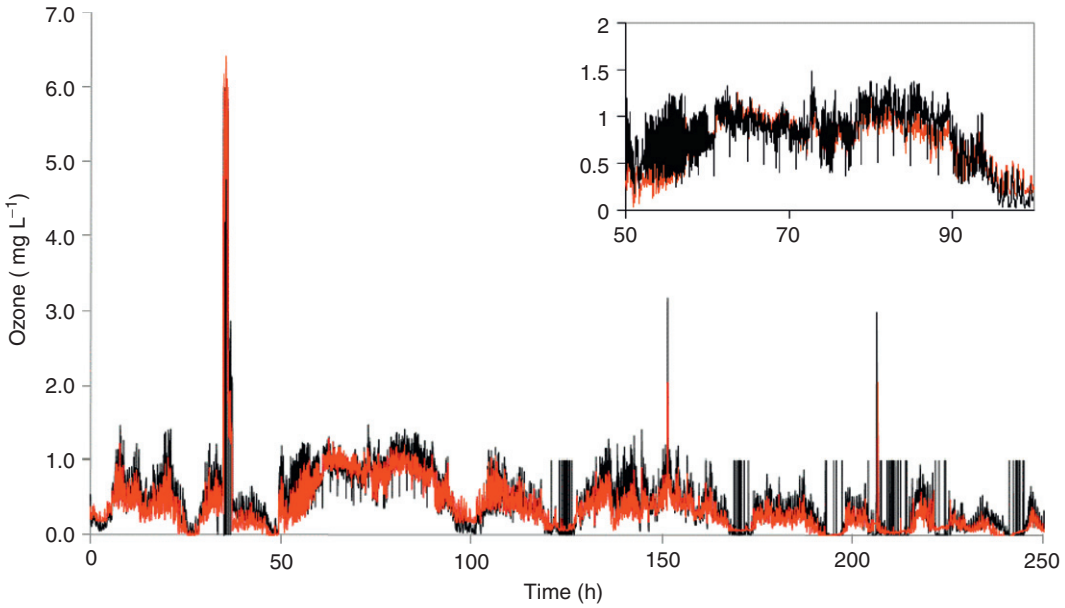

Figure 5 Overlaid of optical (red) and electrochemical (black) ozone sensor measurements in wastewater. Data courtesy of S::can Messtechnik GmbH.

Table 10 Some commercial sensors for waterborne ozone measurements

Transduction principle	*Model*	*Dynamic range (mg l^{-1})*	*Precision*	*LOD (μg l^{-1})*	*Response time (s)*	*Temp. range (°C)*
Amperometric	DULCOTEST®[a]	0.05–2	0.01 ppm	NA	5	0–40
Amperometric	Q45H/64[b]	0–200	0.5%	NA	NA	−20–60
UV-VIS absorption	spectro::lyser™[c]	0–30	0.015 ppm	NA	NA	5–40
UV-VIS absorption	dFFOZ-W[d]	0–150	1%	NA	NA	NA
Amperometric	DOM-1[e]	0–2	10%	30	60	20–30
Amperometric	CRIUS 4800[f]	0–10	±5%	1	1800	0–40
Amperometric	9185sc Ozone Sensor[g]	0–2	3% or ±10 ppb	5	90	0–45
UV-VIS absorption	OZ-96[h]	0–100	±0.5 ppm	NA	NA	5–30
Amperometric	OZ-50[i]	0.1–10	±3%	NA	<60	5–40

[a]ProMinent Dosiertechnik GmbH (http://www.prominent.de).
[b]Analytical Technology Inc. (http://www.analyticaltechnology.com).
[c]S::can Messtechnik GmbH (http://www.s-canat).
[d]IN USA Inc. (http://www.inusacorp.com).
[e]Eco Sensors Inc. (http://www.ecosensors.com).
[f]Process Instruments (UK) Ltd. (http://www.processinstruments.net).
[g]Hach Co. (http://www.hach.com).
[h]HORIBA Advanced Techno (http://www.horiba.com).
[i]Bionics Instrument (http://www.bionics-instrument.com).
NA, not available.

end, sensors based on the characteristic immiscibility of hydrocarbons and water have been developed. On the other hand, environmental protection agencies concentrate their efforts in detecting low levels of hydrocarbons in drinking water or recreation areas. A similar target is aimed at by the naval industry through the International Maritime Organization (IMO), whose Marine Environment Protection Committee has established an upper limit of 15 mg l^{-1} for the oil pollution by ships and mandates control of the emission to the oceans by installation of alarm systems (IMO resolution MEPC 107[49]). Therefore, careful consideration of the sought application for the hydrocarbon-sensing device is the first step to making the right choice of the monitoring technology. Moreover, some of the marketed sensors (see ahead) do not discriminate among the different hydrocarbon types and volatile organic compounds (e.g., chlorinated hydrocarbons). These hydrocarbons-in-water sensors are reviewed here according to their technology rather than the exact targeted analyte.

3.10.7.1 Oil-Spill Detection

Since most hydrocarbons have low solubility in water and their density is lesser than 1, the presence of relatively large amounts of hydrocarbon in water is manifested as an oily

layer on the water surface. Such a situation has been used, for instance, by GE Analytical Instruments Inc. (Boulder, CO, USA) for developing the Leakwise® oil-spill sensor. It is a floating device that continuously monitors the liquid surface using a high-frequency electromagnetic absorption technique. Since water absorbs more electromagnetic energy than hydrocarbons, changes in the absorption rate of water indicate the presence or buildup of a hydrocarbon layer. The sensor uses a frequency of 2.45 GHz where the effect of the difference between the water and hydrocarbon dielectric constants is maximum and the influence of salinity is greatly reduced. This sensor has a detection range of 0.3–25 mm oil layer but, being a floating device, it has operational limitations when the water-level variations or lateral currents are too high. Another floating hydrocarbon sensor is the 2114 HCF from Arjay Engineering Ltd. (Oakville, ON, Canada) that monitors the capacitance field between the probe and its concentric shield. As the volume of separated oil increases over the water surface, the probe capacitance changes.

Conductivity sensors based on the large difference between dielectric constants of water and hydrocarbons have also been developed. The Expo Instruments Cobra monitor (Sunnyvale, CA, USA) has a conductive polymer that changes its resistance when hydrocarbons are adsorbed. Conductivity measurements are also the basis of the Waterra HS-1 sensor (Bellingham, WA, USA) to make inspections in narrow wells. An additional measurement with an ultrasonic sensor offers the possibility of determining the thickness of the hydrocarbon layer over the water.

The sensing devices mentioned above are useful for detection of large amounts of hydrocarbon spills at a particular point. However, they may be insufficient for environmental protection agencies that have the mission of monitoring vast water areas. Two different strategies have been adopted to tackle this problem: (1) installation of several oil point detectors and (2) development of systems for very large surface surveillance. The latter has usually been realized by installing detectors in an aircraft that can scan a large area in a short period of time, searching for an oil spill.

Hydrocarbon layers, which are optically thick fluids, absorb solar radiation and re-emit a portion of this radiation as thermal energy, primarily in the IR region (8000–14 000 nm or 1250–700 cm^{-1}). Therefore, during daylight, IR-based sensing devices do not need an excitation source to operate, an advantage in terms of cost and size against other optical sensors. However, IR sensors cannot detect oil-in-water emulsions under most circumstances and several factors can interfere with the measurements including seaweeds and the shoreline.

Aromatic hydrocarbons, particularly those containing multiple condensed rings, are strongly fluorescent (Figure 6). Both, the characteristic spectral (excitation/emission) and decay features of the fluorescence can be monitored and correlated to the particular hydrocarbon for quantitative and forensic measurements, very often with the aid of chemometrics. Unfortunately, the fluorescence intensity of an oil spill in seawater, excited by sunlight, is *c.* 5 times lower than that required for detection. Therefore, unlike IR sensors, optical fluorosensors require the use of lasers operating in the ultraviolet (300–355 nm) or visible (488 nm, e.g., Ar ion) for excitation of the pollutant. For instance, the FLS® Fluorescent LIDAR System of Laser Diagnostic Instruments AS (Tallin, Estonia) can monitor vast territories and detect hydrocarbon pollution at ppm level in water.

Airborne oil-spill detection systems working on the principle of scattering of low-frequency electromagnetic radiation are also commercially available. The interaction between microwave radiation and the waves generated by the wind on the ocean surface, results in a scattered radiation known as Bragg scattering. The presence of an oil layer on the ocean surface reduces sea-surface roughness and dampens wind waves. Therefore, the back-scattered radar power decreases, creating dark structures in the radar images that signal the polluted area. This is the principle of SeaDarQ BV (Hardinxveld-Giessendam, The Netherlands) and Miros AS (Asker, Norway) large oil-spill detection systems.

3.10.7.2 Water-Quality Control

When the level of waterborne hydrocarbons lies in the mg l^{-1} (ppm) or μg l^{-1} (ppb) ranges, no oil layer builds up and the pollutants are either dissolved or suspended as micro-droplets. In these two situations, optical sensors may be the best choice.

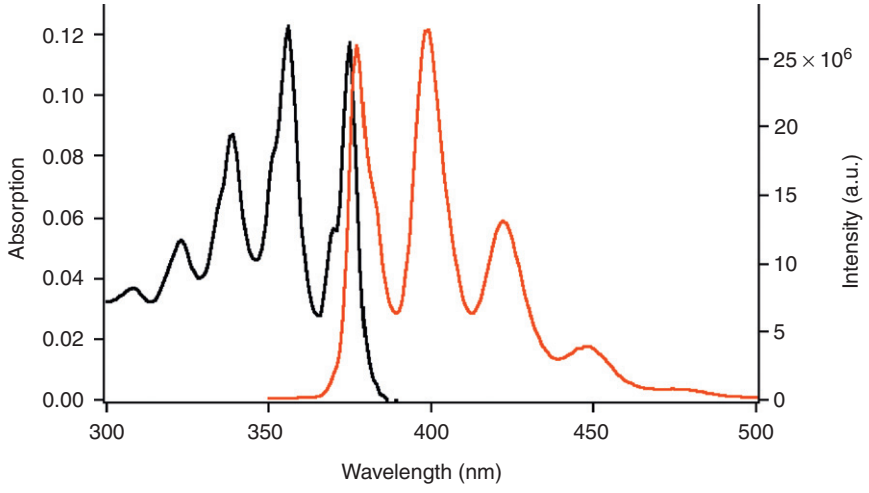

Figure 6 Absorption and emission ($\lambda_{exc} = 340$ nm) spectra of anthracene.

The most intuitive method to develop an optical hydrocarbon sensor is to use the intrinsic photophysical properties (absorption and/or emission of light) of the analyte itself. Aromatic hydrocarbons absorb strongly in the UV spectral region and both aromatic and aliphatic hydrocarbons display characteristic (narrow) absorption bands in the IR region. Aromatic hydrocarbons also display strong fluorescence that may be employed for more sensitive direct sensing as has been shown earlier. The difference of refractive index between water and hydrocarbons may also be the basis for alternative optosensing schemes. Moreover, some sensors capitalize on the light-scattering properties of the hydrocarbon micro-droplet suspensions in water to determine the pollutant concentration. In general, interferences from the matrix (e.g., strongly absorbing media or high levels of suspended particles) are bound to affect the performance of the above-mentioned optical sensors profoundly for waterborne hydrocarbon measurements (but not of indicator-mediated ones, see Section 3.10.7.2.4).

3.10.7.2.1 Sensors based on refractive-index changes

The adsorption of hydrocarbons onto the cladding of a polymer-coated silica (PCS) optical fiber provokes a change in refractive index and therefore in the intensity of the light transmitted along the fiber by attenuated total reflection. This is the basis, for instance, of the fiber-optic chemical sensor developed by Petrosense Inc. (Las Vegas, NV, USA) CMS-4000.

A popular class of fiber-optic sensors based on refractive-index changes uses the so-called fiber Bragg gratings (FBGs) and long-period gratings (LPGs) as the analyte-sensitive device. In both cases, thanks to a periodic variation in the refractive index made to the fiber core, a selection of transmitted wavelengths is obtained. The latter shift upon a change in the grating refractive index, due to adsorption of the hydrocarbons. Nevertheless, depending on the adsorbent polymer and the monitored hydrocarbon type, reversibility of the refractive-index-based fiber-optic sensors may be an issue. Therefore, instrument manufacturers offer optional sensor-cleaning systems.

3.10.7.2.2 Sensors based on light scattering

The scarce solubility of hydrocarbons in water usually leads to micro-droplet formation even at ppm concentrations that produce scattering of the incident light (see Section 3.10.13). For instance, Dexil Corp. (Hamden, CT) PetroFLAG® is an off-line hydrocarbon analyzer that includes extraction, filtration, and turbidity measurements to determine hydrocarbons in water samples. Multiwavelength light scattering (MWLS) with detection at different angles is used by Deckma GmbH (Hamburg, Germany) in their online OMD-7 MKII hydrocarbon detector, specially designed for installation on board ships for monitoring ocean pollution. Measurements at three different wavelengths and various angles of detection allow obtaining turbidity, and oil and solid concentrations with the same equipment. MWLS including the near-IR (NIR) region is used by Rivertrace Engineering Ltd. (Redhill, Surrey, England) in the OCD Xtra oil-in-water analytical system. Both the OMD-2005 monitor of DVZ Services GmbH (Syke, Germany) and the TF16-EX sensor of Optek-Danulat GmbH (Essen, Germany) use combined light scattering and VIS–NIR absorption data for determination of oil concentrations in water. In general, sensors based on light-scattering measurements are strongly affected by suspended particles present in the sample. In particular, iron-oxide particles have been identified as the major source of interference in sensors installed on ships, and some manufacturers have developed special systems for their elimination or discrimination to avoid false-positive alarms of hydrocarbon presence in the water.

3.10.7.2.3 Sensors based on absorption changes

The UV absorption of aromatic hydrocarbons has been used for the development of rugged optical sensors. For instance, S::can Messtechnik GmbH (Vienna, Austria) manufactures the Spectro::lyser system that measures the absorption between 220 and 390 nm to determine the concentration of benzene, toluene, ethylbenzene, and xylene (BTEX). It is a double-beam instrument that compensates light scattering from suspended solids, with a variable path length from 1 to 100 mm depending on the analyte and sensitivity required. Optek-Danulat GmbH (Essen, Germany) offers its AF46-EX, a dual-channel UV absorption (254, 280, 290, 300, and 313 nm) sensor with optical paths from 1 to 500 mm. The Teledyne Analytical Instruments (City of Industry, CA) 6600 model includes an *in situ* ultrasound homogenizer to dissolve the oil in water before UV-absorption analysis and minimize interferences from scattering. Dissolved natural organic matter or UV-absorbing salts are other potential sources of interference.

The use of NIR sensors for *in situ* water-quality control is limited by the strong absorption of water in these regions due to the combination and overtone O–H absorption bands. These bands are often stronger than the C–H absorptions of hydrocarbons, impairing direct determination of the latter in aqueous medium. Therefore, traditional (off-line) hydrocarbon-determination methods based on NIR spectroscopy must include a previous extraction step with freon (American Society for Testing and Materials (ASTM) Method D3921) or, nowadays, more environmentally acceptable solvents such as S-316 (ASTM Method D7066-04). An example is the portable InfraCal® analyzer from Wilks Enterprise, Inc. (South Norwalk, CT, USA). Nevertheless, this procedure has particular interest for analyses where online monitoring presents special difficulties due to the presence of high levels of suspended solids or for the analysis of hydrocarbons in soil. Some online sensing devices do both extraction and analysis, with a 5–30 min operational delay. For instance, Horiba's OCMA-25 (Northampton, UK) includes extraction of waterborne hydrocarbons with S-316 and absorbance measurements in the IR region (3400 nm).

The solvent-extraction step can be eliminated using spectroscopic techniques based on evanescent field absorption (EFA) measurements using polymer-coated optical fibers as the sensing elements and the NIR or mid-infrared (MIR) spectral ranges. The latter type of hydrocarbon sensors could only be developed after the appearance of silver halide-based optical fibers which display high transmission in the IR region. The EFAS® fiber-optic sensor for *in-situ* monitoring of organic pollutants in water from Siegrist (Karlsruhe, Germany) capitalizes on the EFA principle. Novel approaches include planar

and liquid-core waveguide technology. On these waveguide-evanescent optical sensors, the coating layer is the key part of the sensor, which determines the selectivity and sensitivity of the final device. Teflon, poly(dimethylsiloxane), polysiloxane with polysiloxane–xerogel, poly(vinyl chloride) (PVC), and low-density polyethylene (LDPE) have all been used to monitor aliphatic, aromatic, and chlorinated hydrocarbons in water.

Inelastic Raman-scattering sensors based on Y-shaped fiber-optic reflection probes have also been used to monitor waterborne hydrocarbons. To improve the inherent low sensitivity associated with Raman measurements and to achieve detection limits in the low ppm range for chlorinated hydrocarbons (<1 ppm for trichloroethylene, 15 ppm for perchloroethylene, 15 ppm for chloroform, and 10 ppm for carbon tetrachloride), surface-enhanced Raman spectroscopy (SERS) has been proposed as an alternative. Nevertheless, to the best of our knowledge, no commercial Raman hydrocarbon sensor is currently available.

3.10.7.2.4 Sensors based on emission changes

As mentioned above, aromatic hydrocarbons display a strong fluorescence in the UV-VIS that has been exploited for the development of sensitive monitors. Lieberman *et al.* (1991) described laser-induced fluorescence via optical fibers to measure the level of petroleum hydrocarbons in real time and *in situ* in seawater. An N_2 laser (337 nm, 1.4 mJ, 800 s^{-1} pulses) was coupled to a 10-m bifurcated silica optical fiber and the fluorescence collected by six other fibers concentrically distributed around fiber undergoing excitation. A photodiode array was used as the detector. With this equipment, emission decays and fluorescence spectra of the seawater could be collected and the levels of hydrocarbons continuously monitored.

Commercial equipment based on the hydrocarbon intrinsic fluorescence has been available for long in the market. For instance, the TD-4100 system from Turner Designs Hydrocarbon Instruments Inc. (Fresno, CA, USA) detects hydrocarbons in a stream of water falling through an open chamber in which fluorescence is measured. No adsorption media or measuring flow cell is used and therefore problems of measuring-time delays, regeneration, and cell cleaning are eliminated. UV fluorescence measurements are also used by DMA Sorption ApS (Vedbæk, Denmark) in their Bilge monitor for hydrocarbons in water, reaching response times below 1 s with equipment installed on board ships. The FPM 605 from J.U.M. Engineering GmbH (Karlsfeld, Germany) and the CX6000 from Awa Instruments (Duluth, GA, USA) are further examples of hydrocarbon sensors for online water monitoring based on fluorescence measurements. In the Hydrosense 2410 from Arjay Engineering Ltd. (Oakville, ON, Canada), water flows down a special UV plate to maximize signal strength and stability of the fluorescence reading.

In general, fluorescence determinations (particularly those based on time-resolved measurements) have the advantage of a lower interference from particles or bubbles that usually provoke false-positive alarms in light-scattering-based equipments. However, since most fluorescence sensors use the intrinsic fluorescence of the analyte itself, hydrocarbons with low fluorescence-quantum yield or no emission at all (e.g., aliphatic or chlorinated) prevent the use of such devices for waterborne hydrocarbon monitoring.

To overcome such problems and manufacture more general detectors, different strategies have been proposed. Development of indirect sensors where an immobilized luminescent indicator dye displays a solvatochromic effect on its emission is one of the most promising strategies. Thus, different luminescent dyes such as Nile Red (White *et al.*, 1996) or a ruthenium complex (Castro *et al.*, 2005) have been successfully used to that end. The latter is the base of the fiber-optic portable hydrocarbon-in-water sensor manufactured and recently commercialized by Interlab IEC (Madrid, Spain) within its line of Optosen™ monitoring systems.

A compilation of representative sensors for waterborne hydrocarbons is listed in Table 11.

3.10.8 Sensors for Waterborne Organic Matter

The level of organic pollutants in the river, reservoir, or wastewater is one of the most widely analyzed parameter because excess contamination of these substances in aquatic environments provokes serious damages to the ecosystem. However, while existing laboratory methods and analyzers are plentiful, there are very few sensors for online *in situ* continuous (or even near real-time) monitoring of the several indices related to the contents of waterborne organic matter (COD, BOD, and TOC, see ahead).

3.10.8.1 Sensors for COD

The COD index is commonly used to indirectly measure the overall amount of organic compounds in water and is expressed in milligrams per liter (mg l^{-1}), which indicates the mass of molecular oxygen consumed per liter of solution in the complete oxidation process. COD measuring systems usually imply the total oxidation of the waterborne organic matter and concomitant measurement of the oxygen consumption for such oxidation. Traditionally, oxidation has been done using a strong oxidizing agent such as potassium permanganate ($KMnO_4$). Currently, off-line test kits with potassium dichromate ($K_2Cr_2O_7$) as oxidizing agent are the most popular and practical for routine applications. COD values are determined by means of a photometric method after digestion (Environmental Protection Agency method 410.4).

COD online monitoring equipment based on traditional chemical oxidants, like TOC sensors, usually display disadvantages that mainly include the measuring delay time and the experimental error due to the partial (instead of full) oxidation of some organic and inorganic matter. To overcome these limitations, more efficient methods such as thermal (1200 °C) or ozone oxidation are included in new commercial equipments (see Table 12). A different system is the PeCOD™ from Aqua Diagnostic (South Melbourne, Australia) that directly measures the photocurrent charge originating from the oxidation of organic species contained in a sample. The photocatalytic oxidation of organic matter takes places in a photoelectrochemical cell with a photoactive electrode (e.g., a layer of titanium dioxide nanoparticles coated on an inert

Table 11 Some commercial sensors for waterborne hydrocarbons

Transduction principle	*Analyzer model*	*Dynamic range (mg l^{-1})*	*Precision*	*LOD (mg l^{-1})*	*Response time (s)*	*Limitations/ interferences*	*Temp. range (°C)*
Electrical resistance	Cobra[a]	NA	NA	NA	5	NA	2–74
High-frequency absorption	Leakwise[b]	0.3–25 mm	NA	NA	NA	NA	0–70
UV fluorescence	TD-4100[c]	NA	±10%	0.001–1000	<10	Fluorescent compounds	0–49
Refractive index change	CMS-4000[d]	0–20 000	±15%	<10	<60	NA	0–50
Solvent extraction + IR absorption	OCMA-25[e]	0–100	±3%	NA	600	None	0–40
Multi-wavelength light scattering	OCD Xtra[f]	0–200	±5 ppm	1	NA	NA	0–50
UV fluorescence	DMA ppm Monitor™[g]	0–40	±10%	<15	1	NA	0–70
Three wavelength, multiangle light scattering	OMD-7 MKII[h]	0–200	±10%	5	10	NA	0–70
Absorption and scattering	OMD-2005[i]	0–30	±2%	2	NA	NA	1–65
Solvent extraction, filtration, and turbidity	PetroFLAG™[j]	10–50 000	±10%	15	900	Off-line system	2–35
Solvent extraction + IR absorption	InfraCal™[k]	2–5000	±0.1%	0.5%	600–900	Off-line system	4–45
UV absorption	Spectro::lyser™ [l]	0–100	±0.3%	0.1 ppm	30	NA	5–40
UV-fluorescence	FPM 605 [m]	0–1000	±1.5%	0.1	<12	NA	10–39
Conductivity and ultrasounds	HS-1[n]	NA	NA	1.5 mm	NA	NA	0–50
UV-fluorescence	Hydrosense 2410[o]	0–500	±0.1	0.1	NA	NA	10–50
UV-fluorescence	CX6000[p]	0–1000	±10%	0.1 ppm	<10	NA	0–50
Capacitance	2114-HCF[o]	0–600 mm	±1 mm	NA	NA	NA	0–50
UV absorption	AF46-EX[q]	Hydrocarbon dependent	< ±1%	< ±0.05%	NA	NA	0–70
VIS–NIR absorption + light scattering	TF16-EX[q]	0.5–500	< ±0.3%	< ±0.05%	NA	NA	0–40
Solvent extraction + IR absorption	HC 9010[r]	0.1–10	0.01 ppm	0.1 ppm	1800	NA	5–20
UV absorption	Teledyne 6600[s]	0–200	±2%	1%	<5	NA	0–50
Gas chromatography + FID detection	Teledyne 4080[s]	0–1000	±2%	0.1 ppm	15	For C1 to C9+	4–43
UV-fluorescence	EnviroFlu-HC[t]	0–200	NA	0.1 ppb	NA	NA	0–40
UV-fluorescence	FLS-LIDAR[u]	NA	NA	NA	NA	NA	NA
Long wavelength scattering	SeaDarQ[v]	NA	NA	NA	NA	NA	NA
Long wavelength scattering	Miros ODS[w]	NA	NA	NA	NA	NA	NA

[a]Expo Instruments Inc. (http://www.expoinstruments.com).
[b]GE Analytical Instruments Inc. (http://www.geinstruments.com).
[c]Turner Designs Hydrocarbon Instruments Inc. (http://www.oilinwatermonitors.com).
[d]Petrosense Inc. (http://www.petrosense.com).
[e]Horiba (http://www.horiba.co.uk).
[f]Rivertrace Engineering Ltd. (http://www.rivertrace.com).
[g]DMA sorption (http://www.dma-sorption.dk).
[h]Deckmahamburg GmbH (http://www.deckma.com).
[i]DVZ group (http://www.dvz-services.de).
[j]Dexil Corporation (http://www.dexsil.com).
[k]Wilks Enterprise Inc. (http://www.wilksir.com).
[l]S::can Messtechnik GmbH (http://www.s-caNAt).
[m]J.U.M. Engineering GmbH (http://www.jum.com).
[n]waterra USA Inc. (http://www.waterra.com).
[o]Arjay Engineering Ltd. (http://www.arjayeng.com).
[p]Awa Instruments (http://www.awa-instruments.com).
[q]Optek-Danulat GmbH (http://www.optek.com).
[r]Environnement S.A. (http://www.environnement-sa.com).
[s]Teledyne Analytical Instruments Inc. (http://www.teledyne-ai.com).
[t]TriOS Mess- und Datentechnik GmbH (http://www.trios.de).
[u]Laser Diagnostic Instruments AS (http://www.ldi.ee).
[v]SeaDarQ B.V. (http://www.seadarq.com).
[w]Miros AS (http://www.miros.no).
NA, not available.

Table 12 Some commercial sensors for the chemical oxygen demand (COD) of water

Oxidation method and transduction principle	*Model*	*Dynamic range (mg l^{-1})*	*Precision*	*LOD (mg l^{-1})*	*Response time (s)*	*Temprature range (°C)*
Heat + O_2 determination	QuickCOD®[a]	0–100	NA	NA	60	NA
Oxidation + photocurrent measurements	PeCOD™ P100 analyzer[b]	0–350	3%	0.2	30–300	NA
UV-VIS absorption	CarbonVIS® 700/1 IQ[c]	0–2500	3%	NA	NA	NA
O_3 oxidation + O_3 differences	Phoenix 1010[d]	0–100 000	5%	10	180–900	5–40
UV_{254} absorption	UV 400[e]	0–20 000	10 ppm	NA	10	0–50

[a]LAR Process Analyzers AG (http://www.lar.com).
[b]Aqua Diagnostic (http://www.aquadiagnostic.com).
[c]WTW GmbH (http://www.wtw.com).
[d]Endress + Hauser Instruments AG (http://www.endress.com).
[e]Tethys Instruments SAS (http://www.tethys-instruments.com).
NA, not available.

conductive substrate) and the changes in photocurrent are related to the COD value. No consumption of an oxidizing agent is involved but an electrolyte solution is needed.

Since most organic compounds absorb in the UV region, the absorption spectra of water samples can yield COD data. No oxidation reagent is consumed as no sample treatment is performed, with consequent saving in time, device size, and system autonomy.

Electrochemical methods have also been successfully applied to laboratory measurements. For instance, COD levels between 20 and 9000 mg l^{-1} have been determined amperometrically with a boron-doped diamond electrode. Oxidation is carried out by the formed hydroxyl radical at the surfaces of the electrode upon water electrolysis. The current of the working electrode changes proportionally with the concentration of the organic matter as long as the physisorbed $HO^{\bullet}$ radicals are not depleted. Another amperometric sensor with a surface ground copper electrode has been used to measure 10–1000 mg l^{-1} COD thanks to the catalytic action of copper.

Table 12 summarizes representative COD sensors for water analysis.

3.10.8.2 Sensors for BOD

BOD, also called biochemical oxygen demand, is another very common index of the quality of water based on quantification of the overall concentration of organic substances by their effect on the respiration of a microbial biomass. The conventional parameter of quality, dating back to 1908, is the so-called BOD-5 (or BOD_5) method that measures the oxygen consumption of a sample at 20 °C over 5 days in the dark, by aerobic microorganisms deliberately introduced into the water sample in a closed container. The rate of oxygen uptake is nowadays measured by an oxygen sensor placed in the headspace. The values of the BOD-5 for the different waters can be accurately measured to comply with legislation but the index is of no use for early warning of environmental damage (spills, runoffs, illegal discharges, etc.), industrial wastewater real-time monitoring, or for maximizing the efficiency of wastewater plant operation (optimization of the biological treatment by monitoring the instantaneous organic-matter level of the influent and the effluent).

To overcome the pitfalls of the BOD-5 method, an electrochemical biosensor for BOD estimation was developed, as early as 1977, based on Karube's work in Japan. The biosensor contains whole microorganism cells immobilized on an acetylcellulose membrane in contact with the water to be measured on the one side, and with a Clark-type oxygen electrode on the other (see Section 3.10.5). While the BOD-5 method uses a mixture of microorganism species, the Karube BOD sensor was based on the respiration of a population of *Trichosporon cutaneum*. The yeast degrades most organic compounds with concomitant decrease of the dissolved oxygen level producing a measurable response of the oxygen sensor. The microbial sensor BOD values linearly correlated with the BOD-5 values in the 0–60 mg l^{-1} range of a glucose–glutamic acid (GGA) standard solution, with a 20-min response time. The sensor was marketed in 1983 (Nissin Electric Co.) and successfully used, for instance, to measure wastewaters from fermentation plants. Only phosphate buffer and GGA solutions were required for the daily measurements.

Several improvements have been introduced in current BOD sensors to reduce their response time (down to 30 s), extend their operational lifetime before change of the sensitive terminal (more than a year), and to raise their sensitivity (limits of detection as low as 0.2 mg l^{-1}). These improvements have been possible thanks to the introduction of flow-injection analyzers (FIAs) to perform automatic water sampling, transport, dilutions and standardization, substitution of luminescent optical oxygen sensors (see Section 3.10.5) for the electrochemical devices, and the replacement of *Pseudomonas putida*, *Pseudomonas fluorescens biovar*, *Bacillus subtilis*, *Stenotrophomonas maltophilia* (among others), or even activated

sludge for the *T. cutaneum*, which is unable to degrade less-biodegradable organic substances.

There are, currently, only a few commercial online BOD analyzers. The Japanese ruggedized BOD 3300 and the benchtop α-1000 models of Central Kagaku Co. are based on the original Karube's electrochemical O_2 sensor respiration measurements to determine BOD levels between 0–500 and 2–50 mg l^{-1}, respectively, every 30–60 min. The Spanish Optosen®-DBO *in situ* analyzer (Interlab Ingeniería Electrónica) uses state-of-the-art luminescent measurements of dissolved O_2 to interrogate respiration of the immobilized microbial biomass. The sensor allows BOD determinations in the 0–2000 mg l^{-1} range every 20–60 min. However, the South Korean company Korbi has opted for a microbial fuel cell to degrade the sample in its online HABS-2000 analyzer, and correlate the generated electrical signal with the water BOD level (0.1–200 mg l^{-1}).

In spite of the potential advantages of *in situ* online BOD sensing, these analyzers are not yet widespread due to (1) the lack of legislation enforcement to perform such measurements, (2) the difficulties often found to relate instant BOD readings with the traditional BOD-5 measurements for water samples with high levels of suspended organic matter, and (3) the recent availability of competing technologies such as TOC online analyzers (see Section 3.10.8.3).

3.10.8.3 Sensors for TOC

TOC is the amount of bound carbon in waterborne organic compounds and is yet another nonspecific indicator of water quality often used as an alternative to COD or BOD measurements. In other to avoid interferences from waterborne inorganic carbon (IC), mainly from carbonate and hydrogen carbonate ions, a previous acidification and purging with inert gas of the water sample is included in some of the equipment. Traditionally, TOC analysis has included a first-digestion stage where both organic and inorganic matter is oxidized to CO_2. Subsequently, the generated CO_2 is quantified and the TOC calculated. A combination of persulfate acid addition, UV irradiation, ozone treatment ,and high temperature combustion (1200 °C) are the most common digesting methods depending mostly on the TOC concentration of the sample (see **Table 13**). The combination UV/persulfate is based on the high oxidation potential of the $SO_4^{-\bullet}$ and $^{\bullet}OH$ radicals produced upon irradiation of $S_2O_8^{2-}$ and H_2O, respectively.

The mineralization step is the limiting process in terms of analysis times. Therefore, most commercial equipments show delay times of the order of several minutes. For very low TOC concentrations, Mettler-Toledo Thornton Inc. (Bedford, MA, USA) and GE Analytical Instruments (Boulder, CO, USA) offer the model 5000 and Check Point TOC sensors, respectively (see **Table 13**) that perform an online vacuum-ultraviolet (VUV) (185 nm) oxidation, reducing the total analysis time to less than a minute. Another current approach for low TOC samples is to digest the organic matter by generation of $^{\bullet}OH$ radicals by electrolysis or photochemical dissociation of water molecules. Such a reagent-free long operational lifetime system, coupled with a gas–liquid separator and a nondispersive infrared (NDIR) analyzer is used by National Aeronautics and

Table 13 Some commercial sensors for waterborne total organic carbon (TOC)

Mineralization and transduction principle	*Model*	*Dynamic range (mg l^{-1})*	*Precision*	*LOD*	*Response time (s)*	*Temperature range (°C)*
UV/heated persulfate + CO_2 IR detection	Series 6700[a]	0–10 000	2%	NA	420	0–40
O_3/$^{\bullet}OH$ + CO_2 IR detection	Series 6700[a]	0–25 000	3%	NA	600	0–40
Combustion + CO_2 IR detection	Series 6700[a]	0–10 000	3%	NA	300	0–40
IR detection	Series 6700[a]	0–10	3%	NA	420	0–40
UV–VIS absorption	ProPS–Kit[b]	0–500	NA	NA	NA	NA
UV/cold persulfate + potentiometric CO_2 detection	COT 9010[c]	0–220	0.01 ppm	0.5 ppm	1800	5–30
UV–VIS absorption	carbo::lyser™ II/III[d]	0–150	NA	NA	NA	0–45
O_3/persulfate + CO_2 IR detection	BioTector® Series 4[e]	0–10 000	3%	NA	360	5–40
UV oxidation + differential conductivity	5000TOCe[f]	0–1	0.05 ppb (<5 ppb) 1% (>5 ppb)	0.025 ppb	<60 s	0–90
UV oxidation + conductivity	CheckPoint[g]	0–1	3%	0.05 ppb	15 s	10–40

[a]Teledyne Technologies Company (http://www.teledyne.com).
[b]TriOS Optical Sensors (http://www.trios.de).
[c]Environnement S.A. (http://www.environnement-sa.com).
[d]S::can Messtechnik GmbH (http://www.s-canat).
[e]Pollution Control Systems Ltd. (http://www.biotector.com).
[f]Mettler-Toledo Thornton Inc. (http://us.mt.com).
[g]GE Analytical Instruments (http://www.geinstruments.com).
NA, not available.

Space Administration (NASA) for TOC analysis in the International Space Station.

After the full oxidation step, detection of the generated CO_2 gas takes places by means of IR absorption (at 2350 cm^{-1} after purging the aqueous CO_2 into the gas phase), potentiometric methods, or differences in conductivity of the water before and after mineralization.

The continuous growth of optical sensors is slowly displacing traditional (mineralization–detection) systems in the TOC sensing field as well. Direct UV-VIS absorption of the dissolved organic and inorganic matter has been used by some companies such as S::can (Vienna, Austria) and TriOS (Oldenburg, Germany) for developing alternative *in situ* TOC sensors. Both analyzers use the entire UV spectral region (210–330 nm) while in other optical equipment, such as the Tethys UV 400 (Meylan, France), only absorption at a single wavelength (usually 254 nm) is monitored with the consequent loss of information. Suppression of the digestion stage dramatically reduces both the analysis time and instrument size, eliminates the consumption of oxidizing reagents, and increases the equipment power autonomy. Nevertheless, these analyzers are limited thus far to low TOC measurements.

Compared to BOD measurements, COD and TOC online analyzers provide faster, more reproducible readings. However, the BOD index is more closely related to natural processes than either COD or TOC values because the former uses microorganisms to determine the level of waterborne organic matter (biodegradable organic matter). Additionally, COD readings are affected by the presence of both oxidizing and reducing inorganic matter and TOC has to be corrected by the IC values (mentioned earlier).

A representative collection of TOC sensors is listed in Table 13.

3.10.9 Waterborne Chlorophyll Sensors

Phytoplankton photosynthetic efficiency is one of the biological signals that rapidly reacts to changes in nutrient availability as well as to naturally occurring or anthropogenic toxins (contaminants) and, therefore, is a useful indicator of the environmental water health. As early as in 1956, P. Latimer considered the yield of *in vivo* chlorophyll *a* fluorescence as an index of the photosynthetic efficiency. The fluorescence yield can be used as an approximation to chlorophyll concentrations and, in fact, some commercial equipments use this simple principle (see Table 14). Removal of interferences from other fluorescence substances and discrimination of the different algal groups (green *Chlorophyta*, blue–green *Cyanobacteria*, brown *Heterokontophyta*, *Haptophyta*, or *Dinophyta*) can be performed using several excitation wavelengths and recording an excitation spectrum characteristic of each group. However, fluorescence per unit chlorophyll is not constant but varies according to the photosynthesis rate and also in response to other factors such as prior exposure to excess irradiance.

Correlations between the photosynthesis rate of algal cultures and the increase of the chlorophyll red fluorescence from the photosystem II in the presence of 3-(3,4-dichlorophenyl)-1,1-dimethylurea (DCMU) were first observed by G. Samuelsson and co-workers in 1977. In the presence of the pesticide, green algae will strongly fluoresce due to the inhibition of the photosynthetic electron transport. A pronounced DCMU-induced emission increase is recorded when the photosynthetic activity is high (growing algal culture), while algae in the stationary phase of growth would be expected to show only a small DCMU-induced increase in fluorescence. Based on the comparison of fluorescence readings in the presence and absence of DCMU and using a

Table 14 Some commercial sensors for waterborne chlorophyll

Transduction principle	*Model*	*Dynamic range ($\mu g\ l^{-1}$)*	*Precision*	*LOD ($\mu g\ l^{-1}$)*	*Temperature range (°C)*
Multiple turnover fluorescence	PhytoFlash[a]	0–100	NA	0.15	−2–50
Fluorescence (exc. 470 nm)	ECO FLNTU[b]	0.01–50	1%	0.01	0–30
Fluorescence	YSI 6025[c]	0–400	0.1 $\mu g\ l^{-1}$	0.1	−20–60
Single turnover fluorescence	FIRe[d]	0.05–100	NA	NA	0–40
Fluorescence (exc. 470 nm)	ECO–FL[b]	0–125	NA	0.01	0–30
Fluorescence (exc. 470 nm)	Manta2[e]	0–500	0.01 $\mu g\ l^{-1}$	0.03	NA
Fluorescence (three exc. wav.)	Algae Torch[f]	0–200	0.2 $\mu g\ l^{-1}$	NA	0–30
Single and multiple turnover fluorescence	Fasttracka II[g]	0–600	2%	NA	−10–40
Single turnover fluorescence	Submersible FL3500/SM[h]	NA	NA	NA	0–55

[a]Turner Designs Inc. (http://www.turnerdesigns.com).
[b]WET Labs, Inc. (http://www.wetlabs.com).
[c]YSI Environmental (http://www.ysi.com).
[d]Satlantic Inc. (http://www.satlantic.com).
[e]Eureka Environmental Instrumentation (http://www.eurekaenvironmental.com).
[f]BBE Moldaenke GmbH (http://www.bbe-moldaenke.de).
[g]Chelsea Technologies Group Ltd (http://www.chelsea.co.uk).
[h]Photon Systems Instruments (http://www.psi.cz).
NA, not available.

parallel flow-through fluorometer, Cullen and Renger developed an online method and defined a fluorescence response index (FRI).

Technical advances in electronics have lead to the development of new modulated techniques where the fluorescence yield of chlorophyll *a* can be determined without addition of any inhibitor agent. By repetitive application of short light pulses of saturating intensity, the fluorescence yield at complete suppression of photochemical quenching is repetitively recorded, allowing continuous plots of the photochemical and non-photochemical quenching. In the dark condition, due to emission quenching by the primary electron acceptor of the photosynthetic process (quinone), a low level of fluorescence emanating from the pigment bed is measured (F_0) with a low intensity (not to drive photosynthesis, and in the absence of solar irradiance), exciting beam. When a dark-adapted sample is exposed to a high-energy single turnover flash (10–100 μs), a single photoreduction of all the primary electron acceptor occurs, and the fluorescence rises from F_0 to a maximum fluorescence level (F_m). Thus, the maximum quantum yield of photochemistry in PSII is given by $(F_m - F_0)/F_m$. The use of multi-turnover systems that generate a longer saturating flash (200–10 000 ms), yields a higher increase in fluorescence due to the more effective photochemical quenching process.

The combination of fluorescence techniques and satellite technology has been demonstrated to be a powerful tool for monitoring evolution of ecosystems (**Figure 7**). In this manner, the water-quality evolution in the Baltic sea, the California current, or the Atlantic ocean have all been studied by satellite fluorescence images of the waterborne cyanobacteria provided, among others, by NASA programs SeaWiFS and MODIS-Aqua.

3.10.10 Sensors for Waterborne Pesticides

Pesticides are anthropogenic chemicals commonly used in agriculture. The increasing concern about groundwater pollution due to the use of these compounds requires a strong effort in order to detect such pollutants using reliable, economical, and rapid methods. Pesticides are toxic substances and some of them (e.g., the organophosphates) are powerful inhibitors of enzymes involved in the nerve functions. They normally display low environmental persistence but have acute toxicity, and therefore, there is a demand for fast-screening methods to detect low concentrations of these pollutants. Strict regulations are being enforced in Europe and other developed areas allowing a maximum concentration of $0.1\,\mu g\,l^{-1}$ of individual pesticide residues in drinking water. Unfortunately, many of the sensors that have been developed do not match such a detection limit but may still be used for other water-sensing applications (rivers, lakes, reservoirs, wastewater treatment plant inlets, consent discharges, rainfall runoff monitoring, etc.).

Currently applied methods for the determination of organophosphates and other pesticides in water are mainly based on gas or liquid chromatographic analyses of water samples, which generally have the advantage of high sensitivity and selectivity. However, they are intrinsically off-line methods and involve several operations such as extraction, homogenization, clean-up of the sample, and concentration and analytical determination. Due to changes in effluent discharge rates as well as dynamic environmental conditions, the aquatic environment is subject to spatially and temporally changing concentrations of pollutants. Sampling-based techniques are usually incapable of tracking these changes and are therefore not suitable for field deployment. Consequently,

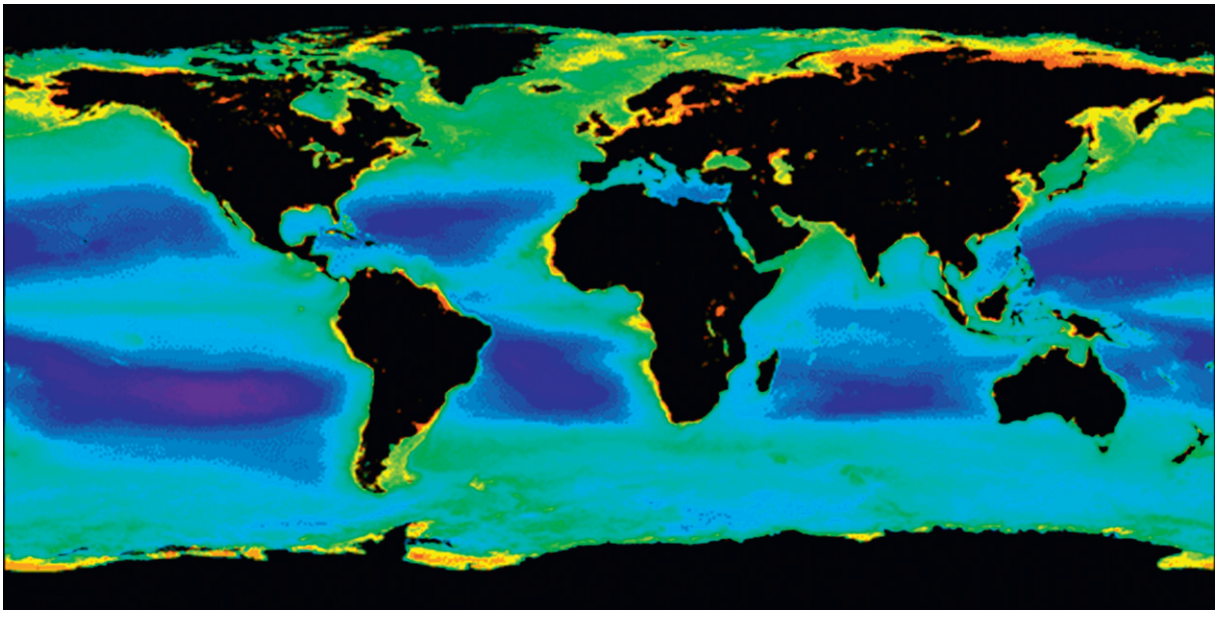

Figure 7 *SeaWiFS* image showing the average chlorophyll *a* concentration from October 1997 to April 2002. Image from the SeaWiFS Image Gallery courtesy of GeoEye.

there is still a need for *in situ* continuously operating sensing devices able to monitor pesticides in water at trace levels. Although different sensors have been proposed for their detection, most of them are only able to operate under the controlled laboratory environment or at best with very short-term *in situ* measurements due to the fragility of the immobilized enzyme, the reagent/catalyst consumption, or insufficient sensitivity for field measurements. Consequently, only a few of them have reached the market so far.

The majority of proposed pesticide sensors rely on either electrochemistry or optical measurements. The most popular electrochemical devices are biosensors based on enzyme-activity inhibition using potentiometry or amperometry as transduction principles. For instance, potentiometric methods for the assay of organophosphorous and carbamate pesticides are based on the inhibitory effect of such chemicals on the acetylcholinesterase (AChE) activity and detection using an electrode of subsequent pH changes caused by acetic acid release in the enzyme-catalyzed reaction:

$$\text{Acetylcholine} + \text{H}_2\text{O}_{\text{AChE}} \rightarrow \text{Acetic acid} + \text{Choline}$$

Other enzymes such as organophosphate hydrolase (OPH) have also been used for sensor fabrication by monitoring the enzyme activity inhibition through amperometric detection of OPH-catalyzed electroactive hydrolysis products.

Fiber-optic biosensors based on immobilized acetylcholinesterase are also known. In this case, acidity changes are monitored using pH-sensitive colorimetric or fluorometric dyes instead of a pH electrode (e.g., Abraxis LLC, Warminster, PA and Severn Trent Services, Ft. Washington, PA commercial kits for detection of aldicarb and dicrotophos pesticides). Alternatively, the enzyme-catalyzed hydrolysis of acetylated luminescent dyes can be followed using high sensitivity in automated optical dosimeters. Optical fiber sensors are of particular interest due to their robustness, remote-sensing capability, and absence of interferences by electromagnetic fields or surface potentials.

Other important group of optical sensors for pesticide determination is that based on measurements of the intrinsic optical properties of the analyte (MIR absorption or native luminescence). The MIR technique is limited when dealing with aqueous solutions of an analyte due to strong background absorption of water in this region. However, fiber-optic evanescent wave spectroscopy (EWS) is a technique that allows *in-situ* MIR absorption spectroscopy in aqueous environments. The optical waveguides provide a rugged and versatile light-delivery system while EWS can provide suitably short path lengths through a highly absorbing medium such as water.

Based on the principle of attenuated total reflection (ATR), a different approach for pesticide sensing using IR spectrometry has been developed by Janotta *et al.* (2003). A nonpolar organically modified sol–gel material is deposited on the optical fiber. If the thickness is 1.7 μm or more, it prevents interaction of the evanescent field with water and also extracts organophosphate pesticides from the solution. With this arrangement, detection limits below 500 ppb, for parathion, fenitrothion, and paraoxon, were attained and sensor measurements could be performed directly in real-life samples such as river waters.

Using the native luminescence of pesticides as an optical parameter, several sensors are found in literature for water analysis (Cápitan-Vallvey *et al.*, 2001; Ruedas Rama *et al.*, 2002; Salinas-Castillo *et al.*, 2004; Dominguez-Vidal *et al.*, 2007).

In the course of the RIver ANAlyzer (RIANA) European project, Mallat *et al.* have developed a pre-commercial prototype based on a fluorescent immunoassay using labeled antibodies for pesticide determination in water (Klotz *et al.*, 1998; Mallat *et al.*, 1999). Nowadays, it is possible to find some commercial optical immunoassays based on absorption measurements for atrazine determination in water (e.g., Abraxis, Beacon Analytical Systems of Saco, ME and Strategic Diagnostics of Newark, DE, USA). In addition to atrazine, the latter two companies offer similar test kits for determination of other pesticides such as carbofuran, 2,4-dichlorophenoxyacetic acid, etc. For rapid qualitative analysis, Silver Lake Research Corporation (Monrovia, CA, USA) markets a colorimetric immunoassay for atrazine and simazine determination in a test-strip format.

Recently, an immobilized microalgae-based fiber-optic biosensor for simazine determination based on chlorophyll-fluorescence monitoring has been described (Peña-Vázquez *et al.*, 2009). Chlorophyll fluorescence increases when toxicants such as simazine inhibit the algal photosystem II (see Section 3.10.9). Alternatively, microalgal biosensors may be based on the inhibition of the photosynthetic function (O_2 production) in the presence of a pesticide or other toxicant. According to this scheme, a novel fiber-optic biosensor can selectively detect simazine at sub-microgram per liter level, using a dual head containing selected toxicant-sensitive and -resistant mutants of *Dictiosphaerium chlorelloides* immobilized on a porous silicone film and luminescent oxygen transduction (Orellana *et al.*, 2009). In this manner, the lack of analyte specificity due to the nonspecific photosystem II response is overcome.

One of the main problems in the development of microbial biosensors is the incorporation of the microorganisms into a suitable matrix that avoids leaching without affecting stability or rendering a significant loss of activity (Gupta and Chaudhury, 2007). Currently, sol–gel films are considered one of the best options to fabricate (reversible) robust optical chemical sensors and biosensors (Jerónimo *et al.*, 2007).

It is also possible to find some commercially available whole-cell biosensors for pesticides and other toxic species in water. Such devices are based on the inhibition of the bioluminescence of *Vibrio fischeri* bacteria by the overall toxicants. These nonspecific sensors are commercialized by companies such as Strategic Diagnostics and Abraxis.

A representative set of examples of pesticide sensors is listed in **Table 15**.

3.10.11 Sensors for Waterborne Toxins

Toxins are poisonous substances produced by living cells or organisms that are active at very low concentrations (Xiang-Hong and Shuo, 2008). Depending on the organism that produces them, toxins can be classified into bacterial toxins,

Table 15 Analytical figures-of-merit of some academic and commercial sensors for pesticide determination in water

Pesticide	*Dynamic range*	*LOD*	*Precision (%)*	*Response time*	*Temperature tested (°C)*	*Interferences*	*Lifetime*	*Transduction principle*	*References*
Butoxycarboxime Trichlorfon Dimethoate Neostigmin	0.1–10 μmol l^{-1} 5–20 μmol l^{-1} 0.5–100 μmol l^{-1} 0.1–10 μmol l^{-1}	NA	1% (RSD)	NA	NA	NA	NA	Electrochemical	[a]
Coumaphos	0.015–0.90 mg l^{-1}	0.002 mg l^{-1}	NA	NA	NA	NA	NA	Electrochemical	[b]
Trichlorfon Aldicarb Methiocarb	0.05–4.0 mg l^{-1} 0.045–5.0 mg l^{-1} 0.2–20 mg l^{-1}	0.04 mg l^{-1} 0.03 mg l^{-1} 0.08 mg l^{-1}							
Chlorpyrifos-oxon	2–8 μg l^{-1}	0.5 μg l^{-1}	4.7	NA	NA	Phosphate buffer	8 days	Electrochemical	[c]
Methyl parathion	$<5\times10^{-6}$ M	4×10^{-7} M	3.9	60 s	RT	Ionic strength	NA	Electrochemical	[d]
Paraoxon	$4.6–46\times10^{-6}$ M	9×10^{-7} M	5.8			pH			
Carbofuran Paraoxon	5×10^{-8}–5×10^{-7} M 5×10^{-7}–5×10^{-6} M	1.5×10^{-8} M 1.1×10^{-7} M	5.8 3.7	NA	NA	NA	NA	Absorbance	[e]
Aldicarb Dicrotophos	0.026–260 mg l^{-1} 0.14–1400 mg l^{-1} (tested ranges)	NA	NA	30 min	NA	Humic and fulvic acids, Ca^{2+}, Mg^{2+}	NA	Absorbance	[f]
Aldicarb Dicrotophos	0.026–260 mg l^{-1} 0.14–1400 mg l^{-1} (tested ranges)	NA	NA	3 min	NA	Humic and fulvic acids, Ca^{2+}, Mg^{2+}	NA	Colorimetric (qualitative)	[g]
Alachlor	5–100 mg l^{-1}	5 mg l^{-1}	NA	15 min	NA	NA	NA	Mid-IR	[h]
Morestan	1.0–200.0 ng ml^{-1}	0.28 ng ml^{-1}	2.9	2 h	RT	Not found	NA	RT phosphorescence	[i]
Thiabendazole	10–800 ng ml^{-1}	2.35 ng ml^{-1}	0.93	NA	20 ± 0.5 °C	α-Naftol	NA	Fluorescence	[j]
Warfarin	2–40 μg ml^{-1}	0.54 μg ml^{-1}	1.26			*o*-Phenylphenol			
Naptalam	8.1–300.0 ng ml^{-1}	8.1 ng ml^{-1}	2.7	NA	20 °C	NA	NA	RT phosphorescence	[k]
Atrazine	0.001–100 μg l^{-1}	0.18 μg l^{-1}	1–9	15 min	NA	Desethylatrazine	NA	Fluorescence	[l]
Simazine	(tested range)	0.10 μg l^{-1}				Deisopropylatrazine			
Atrazine	0.1–5 μg l^{-1}	0.06 μg l^{-1}	3.5–15.2 (RSD)	15 min	NA	Desethylatrazine	NA	Absorbance	[m]
Atrazine	0.1–5 μg l^{-1}	NA	3.9–22.8 (RSD)	20 min	NA	Desethylatrazine	NA	Absorbance	[n]
Atrazine	0.1–5 μg l^{-1}	0.1 μg l^{-1}	2.6–16.7 (RSD)	50 min	RT	Desethylatrazine	NA	Absorbance	[o]

Atrazine	$\geq 3\,\mu g\,l^{-1}$	NA	NA	10 min	RT	Not found	NA	Colorimetric (qualitative)	[p]
Simazine	$\geq 4\,\mu g\,l^{-1}$								
Simazine	19–860 $\mu g\,l^{-1}$	3.6 $\mu g\,l^{-1}$	5.6	30 min	NA	Atrazine, propazine, terbuthylazine, linuron	3 weeks	Fluorescence	[q]

[a]Wollenberger *et al.* (1994).
[b]Ivanov *et al.* (2002).
[c]Hildebrandt *et al.* (2008).
[d]Wang *et al.* (1999).
[e]Andres and Narayanaswamy (1997).
[f]Organophosphate/Carbamate Screen Kit (http://www.abraxiskits.com).
[g]Eclox Pesticide Strips (http://www.severntrentservices.com).
[h]Walsh *et al.* (1996).
[i]Capitan-Vallvey *et al.* (2001).
[j]Ruedas Rama *et al.* (2002).
[k]Salinas-Castillo *et al.* (2004).
[l]Mallat *et al.* (1999).
[m]Atrazine ELISA Kit (http://www.abraxiskits.com).
[n]Atrazine Tube Kit (http://www.beaconkits.com).
[o]Rapid Assay Kit (http://www.sdix.com).
[p]Watersafe Pesticide Test Strip (http://www.silverlakeresearch.com).
[q]Peña-Vázquez *et al.* (2009).
NA, not available; RT, room temperature.

mycotoxins, and invertebrate and vertebrate toxins. Due to their high toxicity, effective analysis techniques are indispensable. The typical method widely used for the detection and quantification of biological toxins is high-performance liquid chromatography (HPLC) with UV, fluorescence, or mass spectrometric detection. These methods provide sensitive and specific analyses but have problems similar to that previously mentioned for pesticide determination (see Section 3.10.10): (1) they are labor intensive and not really suitable for screening large numbers of samples; (2) the extraction and cleanup processes involve numerous time-consuming steps; and (3) derivatization reagents have been used for converting the toxins into the correspondent fluorescent derivatives, which is a complex procedure and needs skilled personnel. For these reasons, rapid, sensitive and specific methods are needed for routine analysis and monitoring of water samples contaminated by these toxins. In this regard, several sensors and biosensors have emerged in the past decade for toxicity analysis.

Several toxicity sensors for drinking-water protection have been evaluated by the US EPA Environmental Technology Verification Program for concentrations at and below the estimated human lethal concentration. Most of them are immunosensors based on the specific high affinity, antibody–antigen binding interactions and optical-detection techniques, such as those developed by Tetracore (Rockville, MD, USA), ADVNT Biotechnologies (Phoenix, AZ, USA), QTL Biosystems (New Kensington, PA, USA), and Response Biomedical Corp. (Vancouver, BC, Canada). Some of them are test strips that indicate the presence or absence of a certain toxin in a preestablished range (ADVNT, Tetracore). Immunosensors display some limitations such as (1) a strong dependence of the antibody-binding capacity under the assay conditions, for example, pH and temperature, and (2) the irreversible nature of the antibody–antigen interaction. A more complete description about fiber-optic immunosensors for waterborne-toxin detection, their different assay formats, and optical-detection techniques can be found in the review by Marazuela and Moreno-Bondi (2002).

Using a fluorescent-labeled amino-acid sequence, PharmaLeads (Paris, France) has developed a test kit for botulinum toxin determination. The company introduces both the fluorogenic label and a quenching substance in the amino-acid sequence and, when botulinum toxin reaches the quenching substance, segmentation occurs generating an intense fluorescence. Another biosensor has been described for aflatoxin B1 determination in river samples based on potentiometric measurements (Marrazza *et al.*, 1999). In this case, the toxin affinity for polynucleotides is measured by its effect on the oxidation signal of the guanine peak of calf thymus DNA immobilized on the electrode surface.

Other types of biosensors used for toxins determination are the cellular structure- and whole-cell-based devices. In this case, the living microorganism or a specific cellular component is used as the biorecognition element. For instance, Abraxis has developed a biosensor based on bioluminescence quenching of *Vibrio fischeri* bacteria, caused by the effect of toxins on their metabolism. The AbraTox Kit responds to global toxicity in water samples and can be used for pesticide determination (see Section 3.10.10) as well. These sensors display advantages such as (1) whole cells or microorganisms are more tolerant to pH or temperature changes; (2) some microorganisms (i.e., bacteria, fungi, yeast, etc.) can be readily isolated from natural sources (river water, sediments, soil, activated sludge, etc.); (3) a single cell can contain all the enzymes and co-factors needed for detection of the analyte; (4) measurement is frequently possible without extensive preparation of the sample, and (5) biosensors can be easily regenerated by letting the cells re-grow. Limitations of this type of biosensors include longer response times and poorer selectivity compared with enzyme-based biosensors, although this feature can sometimes be turned into an advantage for certain applications (e.g., toxicity screening), as in the case of the Abraxis sensor.

Representative biosensors for toxin-in-water detection can be found in **Table 16**. True sensor devices for waterborne toxins are still lacking but most applications (particularly bioterrorism early alert and detection) can be fulfilled with disposable dosimeters (see Section 3.10.1).

3.10.12 Sensors for Waterborne Bacteria

Development of sensors for real-time detection of bacterial contamination in water supplies is a top but highly challenging priority. For this application, sensors should be sensitive enough, rapid, and robust with long operational lifetime (Ji *et al.*, 2004). Until now, a significant number of detection methods have been developed using the optical, electrochemical, biochemical, and physical properties of the microorganisms (Hobson *et al.*, 1996). Some of them have been commercialized, for example, those based on impedance measurements (Don Whitley Scientific, West Yorkshire, UK; Sy-Lab, Neupurkersdorf, Austria, and BioMerieux, Marcy l'Etoile, France). However, these methods are nonspecific, respond not only to bacteria but to all types of microorganisms present in the water sample, and are time consuming because they are based on microorganism growth.

One rapid unspecific colorimetric method for total bacteria determination is that proposed by Palintest (Kingsway, Team Valley, England). Their test strips comprise nutrient agar for total aerobic count of bacteria and triphenyl tetrazolium chloride (TTC) dye which stains most colonies red for easy enumeration. The range of detection for bacteria is 10^3–10^7 colony-forming units (CFU) ml^{-1} in water. Other types of biosensors have been developed recently for bacteria determination in water samples; these devices are sensitive, specific, and rapid in comparison to the previously cited methods. Some representative examples described in the literature are presented below.

Optical bacteria sensors based on fluorescent nucleic acid stains, acting both as molecular-recognition elements and fluorescent reporters, have been described (Ji *et al.*, 2004; Chuang *et al.*, 2001; Chang *et al.*, 2001). The working principle of these sensors is that the fluorescence quantum yield of some nucleic acid stains significantly increases upon binding to nucleic acids. This signal increase can be correlated to the amount of nucleic acid present in the sample. Since all organisms contain nucleic acids, these sensors are not specific and respond to all bacterial species.

Table 16 Some academic and commercial sensors for toxin determination

Toxin	*Tested range*	*LOD*	*Precision*	*Response time*	*Interferences*	*Transduction principle*	*References*
Anthrax	200–10^{10} spores ml^{-1}	2×10^4 spores ml^{-1}	NA	$\approx$5 h	Humic and fulvic acids, Ca^{2+}, Mg^{2+}	Absorption	[a]
Botulinum A and B	0.004–0.3 mg l^{-1}	0.004 mg l^{-1}					
Ricin	0.0015–15 mg l^{-1}	0.0015 mg l^{-1}					
Botulinum A	5×10^{-5}–0.3 mg l^{-1}	5×10^{-5} mg l^{-1}	NA	NA	Ca^{2+}, Mg^{2+}	Luminescence	[b]
Ricin	5×10^{-5}–15 mg l^{-1}	5×10^{-5} mg l^{-1}					
Anthrax	200–5×10^6 spores ml^{-1}	10^5 spores ml^{-1}	NA	5 min	Ca^{2+}, Mg^{2+}	Fluorescence	[c]
Ricin	0.05–15 mg l^{-1}	0.05 mg l^{-1}					
Anthrax	200–10^{10} spores ml^{-1}	4×10^5 spores ml^{-1}	NA	$<$15 min	Humic and fulvic acids, Ca^{2+}, Mg^{2+}	Fluorescence	[d]
Botulinum A	0.5–25 mg l^{-1}						
Botulinum B	0.3–1000 mg l^{-1}	0.5 mg l^{-1}					
Ricin	1–50 mg l^{-1}	1 mg l^{-1}					
Anthrax	200–10^{10} spores ml^{-1}	10^6 spores ml^{-1}	NA	15 min	Humic and fulvic acids, Ca^{2+}, Mg^{2+}	Colorimetric (qualitative)	[e]
Botulinum A	0.5–25 mg l^{-1}	0.4 mg l^{-1}					
Botulinum B	0.3–1000 mg l^{-1}	0.4 mg l^{-1}					
Ricin	0.4–2000 mg l^{-1}	0.4 mg l^{-1}					
Anthrax	200–10^{10} spores ml^{-1}	10^5 spores ml^{-1}	NA	15 min	Humic and fulvic acids, Ca^{2+}, Mg^{2+}	Colorimetric (qualitative)	[f]
Botulinum A and B	0.01–0.5 mg l^{-1}	0.01 mg l^{-1}					
Ricin	0.035–15 mg l^{-1}	0.035 mg l^{-1}					
Botulinum A	0.01–0.5 mg l^{-1}	0.01 mg l^{-1}	NA	30–60 min	Humic and fulvic acids, Ca^{2+}, Mg^{2+}	Fluorescence	[g]
Botulinum B		0.01 mg l^{-1}					
Aflatoxin B1	10–30 mg l^{-1}	10 mg l^{-1}	NA	2 min	NA	Electrochemical	[h]
Botulinum B	0.0003–0.3 mg l^{-1}	NA	$\leq$34%	60 min	Zn^{2+}, Fe^{2+}, Cu^{2+}	Bioluminescence	[i]
Ricin	0.015–15 mg l^{-1}		$\leq$27%				

[a]Enzyme-linked immunosorbent assay (ELISA) (http://www.tetracore.com).
[b]Bioveris (now within Roche) BioVerify Test Kits and M-Series M1 M Analyzer.
[c]QTL Biosensor (http://www.qtlbio.com).
[d]RAMP Immunoassay Test Cartridges (http://www.responsebio.com).
[e]BADD Immunoassay Test Strips (http://www.advnt.org).
[f]BioThreat Alert Immunoassay Test Strips (http://www.tetracore.com).
[g]EzyBot® A and EzyBot® B Test Kits (http://www.pharmaleads.com).
[h]Marazza *et al.* (1999).
[i]AbraTox Kit (http://www.abraxiskits.com).
NA, not available.

Specific biosensors for bacteria determination have been developed using RNA and DNA probes. Combined with the polymerase chain reaction (PCR, Belgrader *et al.*, 1999), several devices with relatively short response times have been marketed (Applied Biosystems, Foster City, CA, USA; Idaho Technology, Salt Lake City, UT, USA; Invitrogen, Carlsbad, CA, USA). If the sequence of bases of a particular part of the DNA molecule is known, then the complementary sequence (probe) can be synthesized and labeled using a fluorescent reporter. The problem with these type of sensors is that they are limited when faced with unknown or genetically modified organisms.

Strategic Diagnostics has commercialized an enzyme-based qualitative biosensor to detect the presence/absence of total coliforms and *E. coli* in water samples. The Colitag™ method capitalizes on the detection of two enzymes, namely β-glucuronidase and β-galactosidase, which are characteristic of *E. coli* and the coliform groups, respectively. Colitag detects total coliforms using the chromogenic substrate *o*-nitrophenyl-β-D-galactopyranoside (ONPG). Upon hydrolysis by β-galactosidase, ONPG produces a distinct yellow color, confirming the presence of coliforms in the sample. For detecting *E. coli*, Colitag utilizes the fluorogenic enzyme substrate 4-methylumbelliferyl-β-D-glucuronide (MUG). Upon hydrolysis by β-glucuronidase, MUG releases 4-methylumbelliferone. The latter reaction product fluoresces when exposed to UV light. The β-glucuronidase enzyme is specific to *E. coli* and observation of fluorescence differentiates this organism from other members of the coliform group. Colitag is able to detect just one CFU of *E. coli* and other coliform bacteria in 100 ml of water fulfilling the legal requirement in developed countries for potable water. Nevertheless, actual levels of bacteria present in drinking waters of less-developed countries or regions may be higher by 3–4 orders of magnitude.

Bacteriophages or phage organisms can be employed as recognition elements to detect deadly bacteria such as *E. Coli* and *Salmonella*. The genetically engineered phages supplied by Biophage Pharma Inc. (Montreal, Canada), are viruses that recognize specific receptors on the surface of bacteria, to which they bind with extreme selectivity and sensitivity. The system works on the basis of monitoring the change in capacitance caused when the target bacteria attach to the sensing interface (Lei *et al.*, 2008). The phages can also be tagged with fluorophores to render them optically responsive, and are immobilized on the surface of an addressable micro-LED array. The LEDs are used to excite the phage organisms and the fluorescence intensity is dependent on the concentration of specific bacteria attached to the phages (Lei *et al.*, 2008b).

The performance of representative sensing devices for waterborne bacteria is listed in Table 17.

3.10.13 Turbidity Sensors

The main areas of application of the water-turbidity measurements lie on cell-density determinations, crystallization monitoring, filtration control, detection of suspended solids, quality testing, and flocculation monitoring. The units given by turbidity instruments are the so-called nephelometric turbidity units (NTUs) but in the sensing field it is also common to use suspended sediment concentrations (SSCs) and particle size distribution (PSD). Among all methods, two are standardized and approved for turbidity determinations of freshwater and brackish water: Nephelometric Method 2130 B and ISO 7027. The attenuation of an IR beam (e.g., 850 nm) or visible radiation in the red region (e.g., 660 nm) is used to avoid interference due to absorption of organic matter dissolved in the water. Another option is to perform a multiwavelength analysis using a white light source and detect any effects due to absorption. To eliminate interference from extraneous light sources, the analytical beam can be pulsed at a rate of several kilohertz.

Light-scattering-based instruments can operate on either of the two principles: transmission and nephelometry. In the transmission mode, the SSC is calculated using the loss of light through a determined optical path. This simple principle was used by P. A. Secchi to develop the first known turbidimeter, back in 1865. In Secchi's method, a circular disk about 30 cm in diameter is lowered from above the water into the water column, and the point at which it disappears from sight is determined. In the nephelometric mode, SSC is calculated by the amount of light scattered by the suspended particles. This scattered light can be measured at 90° (90° nephelometry) or at 30° ± 15° to the incident beam (backscattering). Depending on the application and the amount of suspended solid, transmission, 90° nephelometry or backscattering is chosen.

Air bubbles are one of the major interferences in these types of systems but can be eliminated applying high pressure (Analytical Technology, Collegeville, PA, USA), introducing a bubble-trap chamber (Hach Co., Loveland, CO,USA), or compensating by statistical treatment of the measured values (Züllig AG, Rheineck, Switzerland). In order to avoid the absorption of light and interference from bubble scattering, acoustic techniques can also be used.

Acoustic measurements of suspended particles in the water are based on two approaches: the first method is to measure the attenuation of an acoustic pulse passing through the water column due to the suspended particles. Particle-size distribution and concentration within the water column can be derived but estimation of distribution, as a function of depth, cannot be inferred. Commercial equipments based on ultrasonic attenuation are currently in the market (e.g., Markland Specialty Engineering Ltd., Georgetown, ON, Canada). The second approach is by interpreting the backscattering, which is the scattering by the suspended particles back to the transducer known as Acoustic Doppler Current Profiler (ADCP). The latter is a state-of-the-art equipment in oceanography and hydrometry for current velocity. The ADCP works by transmitting pings of sound at a constant frequency into the water. As the sound waves travel, they ricochet off particles suspended in the moving water, and reflect back to the instrument. Due to Doppler effect, sound waves bouncing back from a particle moving away from the profiler have a slightly lowered frequency when they return. Particles moving toward the instrument send back higher frequency waves. This shift is used to calculate how fast the particle and the water around it are moving, while the intensity of the signal echoed by the suspended particles contains information on concentration.

This technique has some intrinsic limitations. First, multifrequency ADCP instruments are needed in order to resolve

Table 17 Some academic and commercial sensors for bacteria quantitation in water

Bacteria	*Tested range*	*LOD*	*Response time*	*Temperature range*	*Interferences*	*Lifetime*	*Transduction Principle*	*References*
Escherichia coli *Bacillus subtilis 23095*	10^4–10^8 cells ml^{-1}	10^4 cells ml^{-1}	5 min	4–48 °C	Not found	7 months	Fluorescence	[a]
Pseudomonas aeruginosa	2.4×10^5–2.4×10^7 cells ml^{-1}	2.4×10^5 cells ml^{-1}	15 min	NA	NA	50 h (operational)	Fluorescence	[b]
Pseudomonas aeruginosa	0–5.4×10^7 cells ml^{-1}	NA	10 min	NA	NA	2 months	Fluorescence	[c]
Erwinia herbicola	5–500 cells	NA	7–15 min	NA	NA	NA	Fluorescence	[d]
Escherichia coli	0.2–10^6 cfu ml^{-1}	10 cfu ml^{-1}	NA	NA	Not found	NA	Fluorescence	[e]
Francisella	2×10^3–5×10^4 cfu ml^{-1}	10^3 cfu ml^{-1}	NA	NA	Humic and fulvic acids	NA	Fluorescence	[f]
tularensis, *Yersinia*	0.28–5×10^4 cfu ml^{-1}				Not found			
pestis, Bacillus	200–5×10^4 cfu ml^{-1}				Not found			
anthracis, Brucella	40–5×10^4 cfu ml^{-1}				Not found			
suis, Escherichia coli	0.2–5×10^4 cfu ml^{-1}				Not found			
Francisella tularensis,	2×10^4–5×10^5 cfu ml^{-1}	10^4 cfu ml^{-1}	$<$10 min	NA	Not found	NA	Fluorescence	[g]
Yersinia pestis	0.28–5×10^3 cfu ml^{-1}	10^2 cfu ml^{-1}						
Bacillus anthracis	200–5×10^5 cfu ml^{-1}	10^4 cfu ml^{-1}						

[a] Ji *et al.* (2004).
[b] Chuang *et al.* (2001).
[c] Chang *et al.* (2001).
[d] Belgrader *et al.* (1999).
[e] TaqMan *E. coli* 0157:H7 Detection System (http://www.appliedbiosystems.com).
[f] R.A.P.I.D. System for the detection of *Francisella tularensis*, *Yersinia pestis, Bacillus anthracis, Brucella suis,* and *Escherichia coli* (http://www.idahotech.com).
[g] PathAlert detection Kits for the detection of *Francisella tularensis*, *Yersinis pestis,* and *Bacillus anthracis* (http://www.invitrogen.com).
NA, not available.

whether changes in echo intensity (EI) are associated with changes in sediment concentration, or changes in particle-size distribution. Luckily, most of the manufacturers already offer multi-frequency equipment (Teledyne RD Instruments, Poway, CA, USA; SonTek/YSI, San Diego, CA, USA). Second, an acoustic surrogate is the relation between particle circumference and ADCP frequency, and an error in SSC estimates has been found to increase as the ratio of particle circumference to acoustic wavelength approaches 1. A third limitation is that ADCPs are designed to detect acoustic frequency changes in current profiles and are less accurate in measuring the amplitude changes associated with EI measurements.

Laser-diffraction instruments exploit the principles of small-angle forward-scattering angles. Thus, the method is mostly insensitive to change in particle color or composition. Sequoia Scientific, Inc. (Bellevue, WA, USA) and Shimadzu Corporation (Kyoto, Japan) provide this type of equipment. For instance, the LISST100X and LISST25X (LIST = Laser In-Situ Scattering and Transmissometry) are equipped with a 670 nm laser. Both record scattering at 32 angles, mathematically invert the readings to get the size distribution, and also scale it to obtain the volume-scattering function (VSF). Their working range is from 1 to 750 $mg\,l^{-1}$ and can be modified by increasing or reducing the optical path since it is a forward-scattering measuring technique. For very high SSC samples, the company has developed the LISST-INFINITIVE model that includes one single sample dilution step (50:1). A range from 1 to 500.000 $mg\,l^{-1}$ is achieved, but no data of a possible delay time on the reading is provided by the manufacturer.

Estimation of SSC from fluid-density values computed from pressure measurements is a strong candidate for monitoring high sediment-laden flowstream. In fact, this inexpensive technology is designed to monitor SSC values over 10 $g\,l^{-1}$ since it is based on simultaneous pressure measurements with two exceptionally sensitive pressure-transducer sensors arrayed at different fixed elevations in a water column. The precision pressure sensors are available from several companies but only Waterlog (a division of design Analysis Associates, Inc., Logan, UT, USA) used them for turbidity measurements. Unfortunately, the system is no longer available. In fact, application of this technique in the field can be complicated by low signal-to-noise ratios associated with low SSC, turbulence, significantly large dissolved-solid concentrations, and water-temperature variations.

Table 18 lists the most representative equipments for turbidimetry currently found in the environmental instrumentation market.

3.10.14 Oxidation–Reduction Potential Sensors

The so-called oxidation–reduction potential (ORP, or simply redox) measures the capacity of an aqueous solution to either release or gain electrons by electrochemical reactions. Oxidation and reduction reactions control the behavior of many chemical species in drinking water, wastewater, and aquatic environments. Therefore, ORP values are used in a manner similar to pH values to determine water quality. ORP values are affected by all oxidizing and reducing agents present in water so that they also are nonspecific measurements.

The ORP is determined by measuring the difference of potential between an inert sensing half-cell (indicator electrode) and a reference half-cell (reference electrode) as in pH measurements. The sensing half-cell (typically platinum) acts as a platform for electron transfer to or from the sample. The standard hydrogen electrode (SHE) is the reference from which all standard redox potentials are determined, and has been assigned an arbitrary half-cell potential of 0.00 V. However, it is fragile and impractical for routine use, and therefore Ag/AgCl and saturated calomel (SCE) reference electrodes are used instead. The latter is nowadays phased out because it contains mercury.

At equilibrium, the ORP is calculated as the emf of the overall galvanic cell:

$$E(\mathrm{ORP}) = [E_0 + (2.3RT/nF) \times (\log[\mathrm{Ox}]/[\mathrm{Red}])] - E_{\mathrm{ref}} \quad (9)$$

where E_0 is the standard potential of the redox system versus SHE, R is the universal gas constant, T is the temperature in Kelvin, n is the number of electrons transferred, F is the Faraday's constant, [Ox] and [Red] are the activities of oxidant and reductant species ,and E_{ref} is the half-potential of the reference electrode at 25 °C. The readout of the ORP sensor is a voltage (relative to the reference electrode), with positive values indicating an oxidizing environment (ability to accept electrons) and negative values indicating a reducing environment (ability to donate electrons).

3.10.14.1 Effect of pH on Oxidation–Reduction Potential Sensors

Some redox reactions are pH-dependent, for example, the reduction of the powerful disinfectant hypochlorous acid (HClO), widely used in water treatment as a by-product of chlorine solutions in water:

$$\mathrm{HClO} + \mathrm{H}^+ + 2\mathrm{e}^- \rightleftharpoons \mathrm{Cl}^- + \mathrm{H_2O} (E_0 = 1.49\ \mathrm{V})$$

In this case, the ORP of water would be

$$E(\mathrm{ORP}) = [E_0 + (2.3RT/nF) \times \log([\mathrm{HClO}][\mathrm{H}^+]/[\mathrm{Cl}^-])] - E_{\mathrm{ref}} \quad (10)$$

where the proton activity $[\mathrm{H}^+]$ shows the ORP dependence on pH. If the redox reaction involved depends on the acidity, the solution pH must be controlled to achieve reliable ORP measurements.

3.10.14.2 Effect of Temperature on ORP Sensors

The ORP is directly dependent on the temperature of the sensing system according to Nernst equation above. The actual temperature effect depends on the ratio of activities of each redox couple present in solution. In most cases, electroactive species in solution are unknown and for this reason, temperature is not compensated in ORP sensors. Proper use of ORP sensors require that their calibration is done at the same temperature at which the measurement will be carried out. For this reason, some vendors provide tables containing the ORP

Table 18 Some commercial sensors for water turbidimetry

Transduction principle	*Model*	*Dynamic range*	*Precision*	*LOD*	*Response time (s)*	*Temperature range (°C)*
Infrared backscattering	AF46 CS[a]	0–200 g l^{-1}	NA	NA	NA	0–55
Infrared 90° nephelometry	A15/76[b]	0–4000 NTU	±5% or ±0.02	NA	NA	0–50
Infrared backscattering	OBS–3+[c]	0–4000 NTU	±2% or 0.25	NA	NA	NA
Red (660 nm) light 90° nephelometry	FilterTrak 660™[d]	0–5 NTU	±3% or ±0.005	0.007 NTU	NA	0–40
White or Infrared light 90° nephelometry	MicroTOL[e]	0–1000 NTU	±5%	0.0001 NTU	NA	0–50
Infrared 90° nephelometry	NTU Digital Sensor[f]	0–4000 NTU	±1%	0.01 NTU	<1	0–50
Infrared absorption and 90° nephelometry	NTU–S10[f]	0–20 NTU	NA	NA	NA	−10–50
Infrared 90° nephelometry	270WQ[g]	0–1000 NTU	±1%	NA	5	−10–50
Laser diffraction	LISST100X[h]	1–750 mg l^{-1}	NA	<1 mg l^{-1}	NA	−10–45
Infrared 90° nephelometry	VisoTurb® 700 IQ[i]	0–4000 NTU	±2%	0.05 NTU	NA	0–60
Infrared 90° nephelometry	6136 Turbidity Sensor[j]	0–1000 NTU	±2% or 0.3	0.1 NTU	NA	NA
Laser diffraction	LATS–1[k]	0–3.2 NTU	NA	0.001 NTU	1	NA
Ultrasonic attenuation	Model 502–IL[l]	1–150 g^{-1}	±5% or 1 g/l	NA	60	1–45
Infrared 90° nephelometry	TU 810[m]	0–4000 NTU	1 NTU	0.05%	10	0–50
Infrared absorption	Turbimax W CUS65-C[n]	0–50 g^{-1}	<1%	NA	NA	0–50
Infrared 90° nephelometry	TML–25[o]	0–4000 NTU	<1%	0.001 NTU	2	0–50
Infrared 90° nephelometry	CT–CENSE™[p]	1–200 NTU	±2%	<0.1 NTU	15	0–50
Three (red, blue, green) wavelengths, three angle (100, 125 and 150°) backscattering	ECO VSF3[q]	0–25 NTU	NA	0.01 NTU	NA	0–30
Infrared 90° nephelometry	EL400[r]	0–100 NTU	±2%	0.01 NTU	NA	0–60

[a]Aquasant AG (http://www.aquasant.com).
[b]Analytical Technology, Inc. (http://www.analyticaltechnology.com).
[c]Campbell Scientific Ltd. (http://www.campbellsci.com).
[d]HACH Company (http://www.hach.com).
[e]HF scientific Inc. (http://www.hfscientific.com).
[f]Neotek-Ponsel (http://www.neotek-ponsel.com).
[g]NovaLynx Corporation (http://www.novalynx.com).
[h]Sequoia Scientific Inc. (http://www.sequoiasci.com).
[i]Wissenschaftlich-Technische Werkstätten GmbH (http://www.wtw.com).
[j]YSI Environmental (http://www.ysi.com).
[k]Shimadzu Corporation (http://www.shimadzu.com).
[l]Markland Specialty Engineering Ltd. (http://www.sludgecontrols.com).
[m]RODI Systems Corporation (http://www.rodisystems.com).
[n]Endress + Hauser Inc. (http://www.endress.com).
[o]Züllig AG (http://www.zuellig.ch).
[p]CENSAR Technologies Inc. (http://www.censar.com).
[q]Wetlab Inc. (http://www.wetlabs.com).
[r]Tethys Instruments SAS (http://www.tethys-instruments.com).
NA, not available.

values for the (calibration) standard solution versus the reference electrode at different temperatures.

3.10.14.3 Frequent Problems with ORP Sensors

ORP sensors can show a sluggish response in environmental waters if the platinum electrode of the probe has been contaminated. Common contaminants include hard-water deposits, oil/grease, or organic matter. It may take days to reach the final ORP value in contaminated sensors and, therefore, the typical time frame of a sampling experiment (<1 h) is not sufficient to provide a correct reading. Naturally, if the electrode contaminant is redox-active, either in itself or because it contains redox-active impurities, the sensor reading will be erroneous until the contaminant is removed.

In clean environmental water, there may be very few redox-active species present and those that are present may be in very low concentration. In many cases, the concentration can be so

low that the redox influence of the species is actually below the detection limit of the method.

Finally, the surface composition of the electrode may not be ideal for the measurements in the selected medium. While platinum ORP electrodes are primarily composed of the metal itself (in a neutral state), it is well known that the surface of the electrode where the redox action takes place is coated with a molecular layer of platinum oxide (PtO). The Pt/PtO ratio can change over time, depending on the medium in which the probe is stored, and thus the electrode surface actually possesses its own potential that can be variable. If this surface potential is similar to the ORP potential of the medium, then the electrode response can be slow.

Representative ORP sensors can be found in Table 19.

3.10.15 Conductivity Sensors

Electrical conductivity or specific conductance (κ) is defined as the ability of a liquid to conduct electricity. It is the reciprocal of resistivity and is measured in Siemens cm^{-1}. Conductivity is extensively used to characterize water supplies for municipal, commercial, hospital, and industrial uses. While individual ions cannot easily be differentiated, conductivity gives a measurement of the total ions present in the sample, reading being proportional to the combined effect of all the ions. Conductivity is sometimes expressed as parts per million of total dissolved solids (ppm TDS) and is used to monitor mineral concentration in some applications.

A large variety of conductivity equipment is now available to measure water quality ranging from ultrapure water (very low conductivity) to concentrated chemical water streams (high conductivity). Representative examples are listed in Table 20.

Conductivity sensors for water analysis use two or four electrodes with a known surface area and are directly placed in the solution or built into a tube or vessel at a specified distance. The cell constant (κ_{cell}) refers to the distance between the electrodes divided by the electrode area. If conductivity is low (very dilute solutions) the electrodes are placed close together and the cell constants are between 0.1 and 0.01 cm^{-1}. If conductivity is high, they can be further apart and the cell constants can reach up to 10 cm^{-1}.

The two-electrode conductivity sensors are based on amperometric measurements. In this case, a known potential difference (ΔV) is applied to the pair of electrodes and the resulting electric current (I) is measured. According to Ohm's law ($I = \Delta V/R$) the resistance of the system (R) can be determined and related to conductivity by the following expression:

$$\kappa = \kappa_{cell}/R$$

Unfortunately, the resistance in this method is not constant; salt deposition on the electrodes due to electrolysis can change it. For low to medium conductivity levels (<2 mS cm^{-1}) this method may be sufficient, but for greater accuracy and for higher conductivities, a potentiometric method is required.

Table 19 Representative academic and commercial sensors for water oxidation–reduction potential (ORP) measurements

Dynamic range (mV)	*Precision*	*Response time*	*Temperature range (°C)*	*Pressure range*	*Lifetime*	*References*
90–450	NA	≈1 s	25	NA	NA	[a]
86–268	±0.31, ±0.42, ±0.49 mV (different ranges)	<30 s	20–25	NA	NA	[b]
−450–1100	±0.25, ±0.5, ±2 mV (different ranges)	NA	0–60	NA	NA	[c]
−2000–2000	±2 mV	NA	0–50	NA	NA	[d]
−500–500	2% (RSD)	NA	0–55	<40 psi (276 kPa)	NA	[e]
−999–999	±1 mV	NA	0–50	NA	NA	[f]
−2000–2000	±30 mV	NA	0–60	NA	NA	[g]
−2000–2000	±1 mV	NA	0–60	<50 psi (345 kPa)	NA	[h]
−700–1100	±0.1% (RSD)	10 s	0–80	0–30 psi (0–207 KPa)	5 years	[i]
−1500–1500	NA	NA	0–100	0–232 psi (0–1.6 MPa)	NA	[j]

[a] Lee *et al.* (2007).
[b] Jang *et al.* (2005).
[c] ORP Sensor (http://www.vernier.com).
[d] HI 504 pH/ORP Controller with Sensor Check (http://www.hannainst.com).
[e] WQ600 ORP Sensor (http://www.globalw.com).
[f] ORP15 ORP/Temperature Instrument (http://www.ysiecosense.com).
[g] P & S series ORP electrode (http://www.ionode.com.au).
[h] 720II ORP Controller (http://www.myronl.com).
[i] CSIM11–ORP (http://www.campbellsci.com).
[j] Orbisint CPS12/CPS12D/CPS13 (http://www.endress.com).
NA, not available.

Table 20 Representative examples of academic and commercial sensors for water conductivity measurements

Measuring range	*Precision*	*Cell constant (cm^{-1})*	*Response time*	*Temperature range (°C)*	*Pressure range*	*References*
1–189 mS cm^{-1}	<7% (RSD)	2.02	NA	NA	NA	[a]
0.01 μS–1 mS (conductance)	±5.6 nS (SD)	NA	160 ms	NA	NA	[b]
0–1999 mS cm^{-1} (different ranges)	NA	0.01–10	NA	0–100	0–2 MPa	[c]
0.02–500 mS cm^{-1}	5%	NA	NA	0–100	0–10 bar (0–1 MPa)	[d]
0.005–7 mS cm^{-1}	10%	NA	NA	0–50	NA	[e]
NA	NA	0.1–10.0	NA	0–70	<7.5 bar (750 KPa)	[f]
0–40 000 μS (conductance)	1%	NA	NA	0–55	50 psi (345 kPa)	[g]
0.0001 μS cm^{-1}–2 S cm^{-1} (different ranges)	1.5%	<0.933	NA	0–130	<14 bar (1.4 MPa)	[h]
0–4999 μS cm^{-1} (different ranges)	0.50%	1.0–10	NA	0–95	NA	[i]

[a]Lario-García and Pallas-Areny (2006).
[b]Li and Meijer (2008).
[c]Conductivity analyzers (http://www.yokogawa.com).
[d]InPro 7100 (http://www.mt.com).
[e]CS547A (http://www.campbellsci.com).
[f]Conductivity sensors (http://www.sensorex.com).
[g]WQ301 (http://www.globalw.com).
[h]WTW (http://www.wtw.com).
[i]YSI 3100/3200 (http://www.ysi.com).
NA, not available.

The potentiometric method for conductivity measurements uses four electrodes: the two outermost electrodes apply an alternating voltage. However, rather than directly measuring the current between these two electrodes, the four-electrode sensor measures the voltage drop across the two innermost electrodes. Operating with a known current condition, the resistance of the solution can be calculated using Ohm's law. Unlike amperometric probes, potentiometric conductivity sensors are not limited by electrolysis and therefore can be used for a wider range of conductivities.

3.10.15.1 Effect of Temperature

Conductivity in aqueous solutions increases with increasing temperature because of higher ion mobility. This dependence is usually expressed as a relative change per °C, commonly as percent per °C; this value known as the slope of the particular aqueous solution. For this reason, conductivity readings are normally referenced to 25 °C. Fortunately, temperature sensors are readily available and can be integrated into the electronic circuitry, it being possible to correct the conductivity value and to bring it to its equivalent value at 25 °C automatically.

3.10.16 Conclusions

The text above proves to the reader that there is no shortage of sensors for water. However, legislation pressure and technology advancements are continuously driving the search for novel rugged monitoring devices capable of detecting increasingly lower analyte levels truly online. Substance-specific monitoring is still a challenge particularly for organic water pollutants due to the vast diversity of chemical structures. Therefore, online monitoring sensors and off-line laboratory techniques, such as chromatography interfaced with mass spectrometry, will continue to coexist for many years to come. Each one fulfils an important mission and they are bound to complement each other. However, only reliable, affordable, robust sensors will provide the expected benefits to the humankind and the environment.

Acknowledgments

We gratefully acknowledge support from the funding institutions that have made possible our research in this area: the Madrid Community Government (IV PRICYT ref. CM-S-505/AMB/0374), the European Regional Development Fund, the European Social Fund, the Spanish Ministry of Science and Innovation (CTQ2006-15610-C02-01-BQU and CTQ2009-14565-C03-01), and the UCM-Banco Santander (GR58-08-910072).

References

Aller RC and Zhu Q (2006) Optical pH Sensor. US Pat. 973,663, 18 May 2006.
Amao Y and Nakamura N (2005) An optical sensor with the combination of colorimetric change of α-naphtholphthalein and internal reference luminescent dye for CO_2 in water. *Sensors and Actuators B: Chemical* 107: 861–865.

Andres RT and Narayanaswamy R (1997) Fibre-optic pesticide biosensor based on covalently immobilized acetylcholinesterase and thymol blue. *Talanta* 44: 1335.

Belgrader P, Benett W, Hadley D, *et al.* (1999) PCR detection of bacteria in seven minutes. *Science* 284: 449–450.

Bellerby RGJ, Olsen A, Johannessen T, and Croot P (2002) A high precision spectrophotometric method for on-line shipboard seawater pH measurements: The automated marine pH sensor (AMpS). *Talanta* 56: 61–69.

Brereton RG (2007) *Applied Chemometrics for Scientists.* Chichester: Wiley.

Brown AP, Koval C, and Anson FC (1976) Illustrative electrochemical behavior of reactants irreversibly adsorbed on graphite electrode surfaces. *Journal of Electroanalytical Chemistry* 72: 379–387.

Burke CS, Markey A, Nooney RI, Byrne P, and McDonagh C (2006) Development of an optical sensor probe for the detection of dissolved carbon dioxide. *Sensors and Actuators B: Chemical* 119: 288–294.

Cápitan-Vallvey LF, Fernandez Ramos MD, Avidad R, and Deheidel MKA (2001) Determination of the pesticide morestan by means of a single-use phosphorimetric sensor. *Analytica Chimica Acta* 440: 131–141.

Castro AM, Delgado J, and Orellana G (2005) Hydrocarbon in water sensing with PTFE membranes doped with a luminescent Ru(II) poly(pyridyl) complex. *Journal of Material Chemistry* 15: 2952–2958.

Chan CM, Fung CS, Wong KY, and Lo W (1998) Evaluation of a luminescent ruthenium complex immobilized inside Nafion as optical pH sensor. *Analyst* 123: 1843–1847.

Chang AC, Gillespie JB, and Tabacco MB (2001) Enhanced detection of live bacteria using a dendrimer thin film in an optical biosensor. *Analytical Chemistry* 73: 467–470.

Cho DH, Chung KC, and Park MY (1998) Hydrogen ion-selective membrane electrodes based on alkyldibenzylamines as neutral carriers. *Talanta* 47: 815–821.

Chuang H, Macuch P, and Tabacco MB (2001) Optical sensors for detection of bacteria. 1. General concepts and initial development. *Analytical Chemistry* 73: 462–466.

Creaser CS, Hutchinson WE, and Stephenson GR (2002) An attenuated total reflectance optrode sensor incorporating infrared-active carbonylmetal probe groups. *Sensors and Actuators B: Chemical* 82: 150–157.

Dominguez-Vidal A, Ortega-Barrales P, and Molina-Diaz A (2007) Environmental water samples analysis of pesticides by means of chemometrics combined with fluorimetric multioptosensing. *Journal of Fluorescence* 17: 271–277.

El-Giar EE-DM and Wipf DO (2007) Microparticle-based iridium oxide ultramicroelectrodes for pH sensing and imaging. *Journal of Electroanalytical Chemistry* 609: 147–154.

Ertekin K and Alp S (2006) Enhanced emission based optical carbon dioxide sensing in presence of perfluorochemicals (PFCs). *Sensors and Actuators B: Chemical* 115: 672–677.

Fenster C, Smith AJ, Abts A, Milenkovic S, and Hassel AW (2008) Single tungsten nanowires as pH sensitive electrodes. *Electrochemistry Communications* 10: 1125–1128.

Flannery D, James SW, Tatam RP, and Ashwell GJ (1997) pH sensor using Langmuir–Blodgett overlays on polished optical fibers. *Optical Letters* 22: 567–569.

Gupta R and Chaudhury NK (2007) Entrapment of biomolecules in sol–gel matrix for applications in biosensors: Problems and future prospects. *Biosensors and Bioelectronics* 22: 2387–2399.

Hobson NS, Tothill I, and Turner APF (1996) Microbial detection. *Biosensors and Bioelectronics* 11: 455–477.

Holm AH, Vase KH, Winther-Jensen B, Pedersen SU, and Daasbjerg K (2007) Evaluation of various strategies to formation of pH responsive hydroquinone-terminated films on carbon electrodes. *Electrochimica Acta* 53: 1680–1688.

Hulth S, Aller RC, Engstrom P, and Selander E (2002) A pH plate fluorosensor (optode) for early diagenetic studies of marine sediments. *Limnology and Oceanography* 47: 212–220.

Ivanov AN, Lukachova LV, Evtugyn GA, *et al.* (2002) Polyaniline-modified cholinesterase sensor for pesticide determination. *Bioelectrochemistry* 55: 75–77.

Jang A, Lee JH, Bhadri PR, *et al.* (2005) Miniaturized redox potential probe for *in situ* environmental monitoring. *Environmental Science and Technology* 39(16): 6191–6197.

Jankowska H, Neffe S, and Swiatkowski A (1981) Investigations of the electrochemical properties of activated carbon and carbon black. *Electrochimica Acta* 26: 1861–1866.

Janotta M, Karlowatz M, Vogt F, and Mizaikoff B (2003) Sol–gel based mid-infrared evanescent wave sensors for detection of organophosphate pesticides in aqueous solution. *Analytica Chimica Acta* 496: 339–348.

Jerónimo PCA, Araújo AN, Conceição BSM, and Montenegro M (2007) Optical sensors and biosensors based on sol–gel films. *Talanta* 72: 13–27.

Ji J, Schanzle JA, and Tabacco MB (2004) Real-time detection of bacterial contamination in dynamic aqueous environments using optical sensors. *Analytical Chemistry* 76: 1411–1418.

Jin WJ, Costa-Fernandez JM, and Sanz-Medel A (2001) Room temperature phosphorescence pH optosensor based on energy transfer. *Analytica Chimica Acta* 431: 1–9.

Kaden H, Jahn H, and Berthold M (2004) Study of the glass/polypyrrole interface in an all-solid-state pH sensor. *Solid State Ionics* 169: 129–133.

Kahlert H (2008) Functionalized carbon electrodes for pH determination. *Journal of Solid State Electrochemistry* 12(10): 1255–1266.

Klotz A, Brecht A, Barzen C, *et al.* (1998) Immunofluorescence sensor for water analysis. *Sensors and Actuators B: Chemical* B51: 181–187.

Lario-Garcia J and Pallas-Areny R (2006) Constant-phase element identification in conductivity sensors using a single square wave. *Sensors and Actuators A: Physical* 132: 122–128.

Lau KT, Shepherd R, and Diamond D (2006) Solid state pH sensor based on light emitting diodes (LED) as detector platform. *Sensors* 6: 848–859.

Lawrence NS and Robinson KL (2007) Molecular anchoring of anthracene-based copolymers onto carbon nanotubes: Enhanced pH sensing. *Talanta* 74: 365–369.

Lee JH, Seo Y, Lim TS, Bishop PL, and Papautsky I (2007) MEMS Needle-type sensor array for *in situ* measurements of dissolved oxygen and redox potential. *Environmental Science and Technology* 41: 7857–7863.

Lei Yao H, Ghafar-Zadeh E, Shabani A, Chodavarapu V, and Zourob M (2008a) CMOS capacitive sensor system for bacteria detection using phage organisms. *Proceedings of the 21st Canadian Conference on Electrical and Computer Engineering,* pp. 877–880.

Lei Yao H, Chodavarapu V, Shabani A, Allain B, Zourob M, and Mandeville R (2008b) CMOS imager microsystem for multi-bacteria detection. *Joint 6th International Northeast Workshop on Circuits and Systems and TAISA Conference,* pp. 137–140.

Lieberman SH, Inman SM, and Theriault GA (1991) Laser-induced fluorescence over optical fibers for real-time *in situ* measurement of petroleum hydrocarbons in seawater. *Oceans* 1: 509–514.

Li JP, Peng TZ, and Fang C (2002) Screen-printable sol-gel ceramic carbon composite pH sensor with a receptor zeolite. *Analytica Chimica Acta* 455: 53–60.

Li X and Meijer GCM (2008) A high-performance interface for grounded conductivity sensors. *Measurement Science and Technology* 19: 1–7.

Li ZZ, Niu CG, Zeng GM, *et al.* (2006) A novel fluorescence ratiometric pH sensor based on covalently immobilized piperazinyl-1,8-naphthalimide and benzothioxanthene. *Sensors and Actuators B: Chemical* 114: 308–315.

Mallat E, Barzen C, Klotz A, Brecht A, Gauglitz G, and Barcelo D (1999) River analyzer for chlorotriazines with a direct optical immunosensor. *Environmental Science and Technology* 33: 965–971.

Marazuela MD and Moreno-Bondi MC (2002) Fiber-optic biosensors – an overview. *Analytical and Bioanalytical Chemistry* 372: 664–682.

Marrazza G, Chianella I, and Mascini M (1999) Disposable DNA electrochemical biosensors for environmental monitoring. *Analytica Chimica Acta* 387: 297–307.

Michie WC, Culshaw B, McKenzie I, *et al.* (1995) Distributed sensor for water and pH measurements using fiber optics and swellable polymeric systems. *Optical Letters* 20: 103–105.

Mills A and Eaton K (2000) Optical sensors for carbon dioxide: An overview of sensing strategies past and present. *Química Analítica* 19(supplement 1): 75–86.

Müller B and Hauser PC (1996) Fluorescence optical sensor for low concentrations of dissolved carbon dioxide. *Analyst* 121: 339–343.

Neurauter G, Klimant I, and Wolfbeis OS (2000) Fiber-optic microsensor for high resolution pCO_2 sensing in marine environment. *Fresenius Journal of Analytical Chemistry* 366: 481–487.

Niu CG, Gui XQ, Zeng GM, Guan AL, Gao PF, and Qin PZ (2005) Fluorescence ratiometric pH sensor prepared from covalently immobilized porphyrin and benzothioxanthene. *Analytical and Bioanalytical Chemistry* 383: 349–357.

Nivens DA, Schiza MV, and Angel SM (2002) Multilayer sol–gel membranes for optical sensing applications: Single layer pH and dual layer CO_2 and NH_3 sensors. *Talanta* 58: 543–550.

Orellana G, López-Rodas MV, Costas E, Haigh D, and Maneiro E (2009) Biosensors Based on Microalgae for the Detection of Environmental Pollutants. PCT Pat. Appl. ES2008000465, 29 January 2009.

Orellana G, Moreno-Bondi MC, Segovia E, and Marazuela MD (1992) Fiber-optic sensing of carbon dioxide based on excited-state proton transfer to a luminescent ruthenium(II) complex. *Analytical Chemistry* 64: 2210–2215.

Oter O, Ertekin K, Topkaya D, and Alp S (2006) Room temperature ionic liquids as optical sensor matrix materials for gaseous and dissolved CO_2. *Sensors and Actuators B: Chemical* 117: 295–301.

Peña-Vázquez E, Maneiro E, Pérez-Conde C, Moreno-Bondi MC, and Costas E (2009) Microalgae fiber optic biosensors for herbicide monitoring using sol–gel technology. *Biosensors and Bioelectronics* 24: 3538–3543.

Poghossian A, Berndsen L, and Schoning MJ (2003) Chemical sensor as physical sensor: ISFET-based flow-velocity, flow-direction and diffusion-coefficient sensor. *Sensors and Actuators B: Chemical* 95: 384–390.

Prissanaroon W, Brack N, Pigram PJ, Hale P, Kappen P, and Liesegang J (2005) Fabrication of patterned polypyrrole on fluoropolymers for pH sensing applications. *Synthetic Metals* 154: 105–108.

Ruedas Rama MJ, Ruiz Medina A, and Molina Diaz A (2002) Use of a solid sensing zone implemented with unsegmented flow analysis for simultaneous determination of thiabendazole and warfarin. *Analytica Chimica Acta* 459: 235–243.

Salinas-Castillo A, Fernandez-Sanchez JF, Segura-Carretero A, and Fernandez-Gutierrez A (2004) A facile flow-through phosphorimetric sensing device for simultaneous determination of naptalam and its metabolite 1-naphthylamine. *Analytica Chimica Acta* 522: 19–24.

Sanchez-Barragan I, Costa-Fernandez JM, and Sanz-Medel A (2005) Tailoring the pH response range of fluorescent-based pH sensing phases by sol–gel surfactants co-immobilization. *Sensors and Actuators B: Chemical* 107: 69–76.

Scholz F, Steinhardt T, Kahlert H, Poerksen JR, and Behnert J (2005) Teaching pH measurements with a student-assembled combination quinhydrone electrode. *Journal of Chemical Education* 82: 782–786.

Schöning MJ, Abouzar MH, and Poghossian A (2009) pH and ion sensitivity of a field-effect EIS (electrolyte–insulator–semiconductor) sensor covered with polyelectrolyte multilayers. *Journal of Solid State Electrochemistry* 13: 115–122.

Schroeder CR, Weidgans BM, and Klimant I (2005) pH fluorosensors for use in marine systems. *Analyst* 130: 907–916.

Szepesvary E and Pungor E (1971) Potentiometric determination of acids and bases with a silicone rubber-based graphite electrode as indicator electrode. *Analytica Chimica Acta* 54: 199–208.

Tabacco MB, Uttamlal M, McAllister M, and Walt DR (1999) An autonomous sensor and telemetry system for low-level pCO_2 measurements in seawater. *Analytical Chemistry* 71: 154–161.

Taboada Sotomayor MP, De Paoli MA, and de Oliveira WA (1997) Fiber-optic pH sensor based on poly(*o*-methoxyaniline). *Analytica Chimica Acta* 353: 275–280.

Vuppu S, Kostov Y, and Rao G (2009) Economical wireless optical ratiometric pH sensor. *Measurement Science and Technology* 20: 1–7.

Walsh JE, MacCraith BD, Meaney M, *et al.* (1996) Sensing of chlorinated hydrocarbons and pesticides in water using polymer coated mid-infrared optical fibers. *Analyst* 121: 789–792.

Walt DR, Tabacco MB, and Utamlal M (2000) Fiber Optic Sensor for Long-Term Analyte Measurements in Fluids.US Pat. 6285807, 4 September 2001.

Wang J, Chen L, Mulchandani A, Mulchandani P, and Chen W (1999) Remote biosensor for *in-situ* monitoring of organophosphate nerve agents. *Electroanalysis* 11: 866–869.

White J, Kauer JS, Dickinson TA, and Walt DR (1996) Rapid analyte recognition in a device based on optical sensors and the olfactory system. *Analytical Chemistry* 68: 2191–2202.

Wiegran K, Trapp T, and Cammann K (1999) Development of a dissolved carbon dioxide sensor based on a coulometric titration. *Sensors and Actuators B: Chemical* B57(1–3): 120–124.

Wolfbeis OS, Kovacs B, Goswami K, and Klainer SM (1998) Fiber-optic fluorescence carbon dioxide sensor for environmental monitoring. *Mikrochimica Acta* 129: 181–188.

Wong LS, Brocklesby WS, and Bradley M (2005) Fibre optic pH sensors employing tethered non-fluorescent indicators on macroporous glass. *Sensors and Actuators B: Chemical* 107: 957–962.

Wróblewski W, Rozniecka E, Dybko A, and Brzózka Z (1998) Cellulose-based bulk pH optomembranes. *Sensors and Actuators B: Chemical* 48: 471–475.

Xiang-Hong W and Shuo W (2008) Sensors and biosensors for the determination of small molecule biological toxins. *Sensors* 8: 6045–6054.

Relevant Websites

http://www.abraxiskits.com
Abraxiskits.

http://www.advnt.org
Advnt Biotechnologies.

http://www.analyticaltechnology.com
Analytical Technology.

http://www.appliedbiosystems.com
Applied Biosystems.

http://www.astisensor.com
ASTi: Advanced Sensor Technologies, Inc.

http://www.beaconkits.com
Beacon Analytical Systems.

http://www.biomerieux.es
Biomerieux.

http://www.biophagepharma.net
BiophagePharma.

http://www.campbellsci.com
Campbell Scientific.

http://www.dwscientific.co.uk
Don Whitley Scientific.

http://www.endress.com
Endress + Hauser.

http://www.environnement-sa.com
Environnement S.A.

http://www.grundfosalldos.com
Grundfos Alldos.

http://www.interlab.es
Grupo Interlab.

http://www.hach.com
Hach.

http://www.hannainst.com
HANNA Instruments.

http://www.horiba.com
HORIBA.

http://www.idahotech.com
Idaho Technology.

http://www.sensafe.com
Industrial Test Systems.

http://www.in-situ.com
In-Situ.

http://www.invitrogen.com
Invitrogen.

http://www.ionode.com.au
Ionode.

http://www.jenway.com
Jenway.

http://www.martekinstruments.com
Martek Instruments.

http://www.merck-chemicals.com
Merck.

http://in.mt.com
Metller Toledo.

http://www.myronl.com
Myron L Company.

http://earthobservatory.nasa.gov
NASA: Earth Observatory.

http://lsda.jsc.nasa.gov
NASA: Life Science Data Archive.

http://modis.gsfc.nasa.gov
NASA: MODIS.

http://oceancolor.gsfc.nasa.gov
NASA: Ocean Color Web.

http://www.nexsens.com
Nexsens Technology.

http://www.nico2000.net
NICO 2000.

http://www.palintest.com
Palintest.

http://www.pharmaleads.com
Pharmaleads.

http://www.presens.de
PreSens.

http://www.qtlbio.com
QTL Biodetection.

http://www.responsebio.com
Response Biomedical Corporation.
http://www.s-can.at
s::can.
http://www.satlantic.com
Satlantic.
http://www.sensorex.com
Sensorex.
http://www.severntrentservices.com
Severn Trent Services.
http://www.silverlakeresearch.com
Silver Lake Research.
http://www.sdix.com
Strategic Diagnostics (SDIX).
http://www.swan.ch
SWAN Analytical Instruments.
http://www.sylab.com
SY-Lab.
http://www.tethys-instruments.com
Tethys Instruments.
http://www.tetracore.com
Tetracore.
http://www.thermo.com
Thermo Fisher Scientific.
http://www.epa.gov
United States Environmental Protection Agency (EPA).
http://www.vernier.com
Vernier Software & Technology.
http://www.globalw.com
Water Instrumentation.
http://www.wtw.com
WTW.
http://www.yokogawa.com
Yokogawa.
http://www.ysi.com
YSI.
http://www.ysiecosense.com
YSI; EcoSense.
http://www.ysilifesciences.com
YSI Life Sciences.